Four-Wave Mixing and Propagation of Laser Beam through Atomic Vapor

A thesis presented by

TAHANI ABDULSALAM KHALIFA

to

The Department Of Physics in the Field Quantum Optics and Laser

For the degree of

Doctor of Physics

Mentor: Professor. DUSAN ARSENOVIC

Institution of Physics, College of Belgrade

Belgrade, 2019

Abstract

This thesis deals about theoretically and experimentally investigates the phenomenon [31] FWM (four-wave mixing) in hot potassium fume by co- propagating probe and pump beams through potassium vapor. We get the FWM by way off resonant for double Λ atomic scheme. The system is phase insensitive parametric amplifier due to the gain is independent on initial phases of pump and probe beams when applied in alkali atom vapor.

Model is semi-classical treatment of FWM processes. Theoretically,in the model, the numerical solution of optical Bloch expressions for density matrix terms of every population and coherence were given, to derive the propagating amplitude wave equations of three conjugate beams, probe, pump, and fields after that [31] we evaluate measured and computed gains various important variables for FWM efficiency. This consists of the angle between the probe and the pump, atomic density, two photon detuning and one photon detuning, potassium density and probe power. There is a correlation between effect of one parameter to the gain, and values of the other parameter.

Acknowledgement

Since this could be my remaining chance to express my gratitude to these people in text, I may be somewhat more effusive in my appreciations. Firstly, I am indebted to thank my supervisor Professor, DUSAN ARSENOVIC, for the constant support in my PhD program, for enormous knowledge, inspiration, and his endurance. His direction assisted me throughout my research and when writing this thesis. He has cheerfully answered my queries, assisted me in a myriad ways in the writing. I least expected to get a better guide and mentor for my PhD study than him. I am very lucky to have found a supervisor who took much care about my work, and who promptly reacted to my queries and questions. Much thanks go to my entire Prof in the zemun institute. In particular, I am grateful to Professor BRANA JELENKOVIC, who took the first glance of my thesis, for the advice, encouragement and guidance he offered all through my course. I specially thank to my relatives. No words can appropriately express the depth of my gratitude to my loving mother and to my deceased father for all of the sacrifices they have made for me. Not forgetting all of my brothers and sisters who lent me a hand in writing, and encouraged me to work hard towards my goal. Immeasurable gratitude to my husband, ABOSHAWESHA, who worked tirelessly with me and was always supportive in the times when there,

was no one to address my questions. Last but not least, I am thankful to my children MOHAMMED, MOLOUD, MAWDA and FATIMA for supporting continuously when developing this thesis and my life at large. Thanks so much to all of you for always being there with me.

Table of Contents

Chapter 1

Chapter 2

Chapter 3

1. Introduction

The expression “four-wave mixing” typically refers to the interaction of four spectrally or spatially separate fields it is abbreviated with the symbol FWM. Since it is recognized as good source of entangled pair of photons, so useful in quantum optics [31] for investigating quantum nature of light quanta, in addition to novel technologies for quantum data. It is applied to investigate both one-photon and two-photon resonances in an element by determining the resonant development since at least one of the frequencies is tuned. Excited state cross sections, generations, and line widths can be determined by tuning the frequencies to numerous resonances in the material [6]. This work explores some areas of non-linear optics which such as the phenomena founded in the relationship between four clear optical fields through the D1 line of potassium atomic vapor. [31] Conversely, potassium is an example of the alkaline element with by far smallest ground state hyperfine splitting (HFS). Diverse systems have been employed in the generation of twin photons, including on-resonant impulsive FWM and double ladder scheme FWM. Particular attention in the double FWM structure comes from the capacity to develop quantum field connections. Increased quantum links is present because non- linearity in such system is generated by coherence effect and “spontaneous free emission” rather than large populations of excited states and saturation [1-9]. FWM in a

dual system, [31] with two input fields (pump and probe), is an atomic system applied in the generation of twin beams. This atomic scheme is that of an ordinary electromagnetically induced transparency (EIT). In addition to FWM under definite conditions, parametric amplifier or system is based on laser detuning, pump power and atomic density will become non-linear FWM. Here will be study experimental and theoretical investigations of effects of pump and probe detuning, one (pump) photon detuning (OPD) and Raman two photon pump and probe detuning (TPD) from HF splitting of K ground state and compare results of the numerical calculations with additional experimental results. Measured and calculated gains for different parameters necessary for FWM efficiency. These are the atomic density, angle between the pump and the probe, pump detuning from the D1 shift, and two photon (pump and probe) detuning with reference to HFS of the ground state. Finding relations between different parameters and gains of twin beams. In addition the model is semi-traditional handling of FWM activities consists of working out Bloch relations for density matrix terms of every group and logic related to the double Λ structure of K atom. Calculated matrix elements for coherences (polarization) are coupled to the amplitudes' propagation expressions for electric fields of probe, pump, and combination. Therefore, model with full mathematical models and without confusing theories and assumptions.

Chapter 1

1.1 Atom – Laser Interaction

The use of light has been a very powerful tool to study the internal structure of atoms. Since absorption of light takes place only when the light frequency is nearly resonant with an atomic shift. However, the purpose of this part is to research on the atom-light interface for the simplest systems. So the straight forward case for considering the contact between light and atoms is that of a dual-stage atom compelled by a logical optical spectrum. This chapter summarizes some of that work.

1.2 The Two-Level Atom Interaction with the Classical Field

For a double-level atom [32] in contact with classical electromagnetic field, the field is assumed to be uni color with angular frequency ω to represent the field because of a laser [16]:

$$\vec{E}(t) = \hat{\epsilon}\, E_0 \mathrm{Cos}(\omega t) \qquad (1.2.1)$$

Where, $\hat{\epsilon}$ is the field's unit polarization vector.

Noting the field at the atom location will be an ignorance on our part about the spatial dependence of the field. This is correct in the long-wavelength calculation or dipole calculation, in which we adopt the assumption that the field's wavelength is much bigger than the diameter of the atom. We can therefore disregard any deviations of the field over the size of the atom. This is by and large suitable for optical shifts, the best to do is to break down the field into its negative- and positive-

spinning terms $\vec{E}^{(+)}$ while $\vec{E}^{(-)}$:

$$\vec{E}(t) = \hat{\epsilon}\frac{E}{2}(e^{-i\omega t} + e^{+i\omega t}) \qquad (1.2.2)$$

$$= \vec{E}^{(+)} e^{-i\omega t} + \vec{E}^{(-)} e^{+i\omega t}$$

$$= \vec{E}^{(+)}(t) + \vec{E}^{(-)}(t)$$

Where $\vec{E}^{(\pm)}$ almost $e^{\mp i\omega t}$

It will be treating the atom as a dual-level atom, which obviously an estimate of a real atom. To be specific, we will take into consideration near-resonant interfaces, to facilitate the propagations to the next levels are insignificant. We will also designate the excited levels and ground as |e> and |g> correspondingly, and we will use $\omega_0$to represent the resonant frequency (i.e., the splitting energy of the pair of states $\hbar\omega_0$) see Fig.1

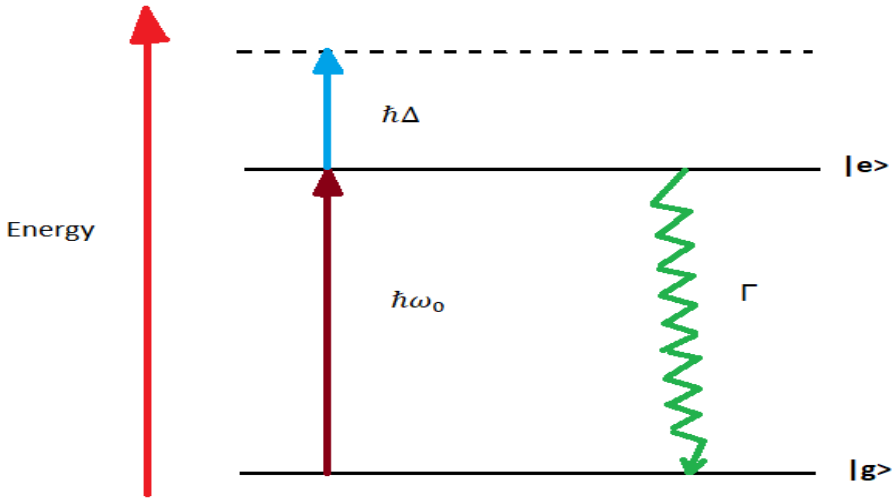

Figure .1: Double level system, with excited - and ground-states |e> and |g>, respectively, with ω_0(a transition frequency) and where the practical light spectrum could have Δ (a detuning). At a characteristic speed Γ, atoms in |e> (the excited state) decay back spontaneously to |g> (the ground state).

The laser field detuning [32] from the atomic resonance defined as, $\Delta = \omega - \omega_0$ we can inscribe the whole Hamiltonian for the field and atom as a quantity of the free $\hat{H}_A$ (atomic Hamiltonian) and the atom–field contact Hamiltonian $\hat{H}_A$:

$$\hat{H} = \hat{H}_A + \hat{H}_{AF} \quad (1.2.3)$$

The atomic free-evolution Hamiltonian can be found by

$$\hat{H}_A = \hbar\omega_0 |e><e| \quad (1.2.4)$$

in taking the ground-state energy to be zero, the $\hat{H}_{AF}$ (atom-field interaction Hamiltonian) in the dipole calculation become

$$\hat{H}_{AF} = -\vec{d}.\vec{E} \quad (1.2.5)$$

Where $\vec{d}$ represents the atomic dipole operator, specified based on r_e(the atomic electron position) as

$$\vec{d} = -er_e$$

Where, r_e is the electron position in relation to the atom.

After compensation for the value of the $\hat{H}_A$ (free atomic Hamiltonian) and the atom-field contact can be written as the total Hamiltonian on the following formula

$$\hat{H} = \hbar\omega_0 |e><e| - \vec{d}.\vec{E} \quad (1.2.6)$$

1.3 Resonance, Absorption is Maximized if Detuning is near zero

We assume that the [32] applied field is denoted by the following equation:

$$\vec{E}(t) = 0.5(\vec{E}_0 e^{i\omega t} + \vec{E}_0^* e^{-i\omega t}). \quad (1.3.1)$$

in which, $\vec{E}_0$ represents the amplitude of electric field. With $\vec{E}$ constant, then the field is nearly resonant with an allowed transition amid the state of atomic ground as well as the state of excite [8-16].

Between the atom and the field, we expect strong collaboration if the atomic transition frequency between the states, $\omega_{eg} = \omega_e - \omega_g$, is close to the driving field's frequency, i.e. $\omega_{eg} \approx \omega$. It is advantageous to transform to new probability amplitudes, which take some trivial oscillation already into account

$$C_e = c_e e^{i(\frac{\omega_e + \omega_g + \omega}{2} t)} \quad (1.3.2a)$$

$$C_g = c_g e^{i(\frac{\omega_e + \omega_g - \omega}{2} t)} \quad (1.3.2b)$$

which leads to the new equations of motion

$$\dot{C_e} = \left[i\left(\frac{\omega_e + \omega_g + \omega}{2}\right) - i\omega_e\right] c_e e^{i(\frac{\omega_e + \omega_g + \omega}{2} t)} + i c_g \frac{\vec{d}_{eg}.\vec{e}}{\hbar} \vec{E}(t)\, e^{i(\frac{\omega_e + \omega_g + \omega}{2} t)} \quad (1.3.3)$$

$$\dot{C_g} = \left[i\left(\frac{\omega_e + \omega_g - \omega}{2}\right) - i\omega_g\right] c_g e^{i(\frac{\omega_e + \omega_g - \omega}{2} t)} + i c_e \frac{\vec{d}_{ge}.\vec{e}}{\hbar} \vec{E}(t)\, e^{i(\frac{\omega_e + \omega_g - \omega}{2} t)} \quad (1.3.4)$$

we introducing the detuning between the electric field frequencies and atomic resonance

$$\Delta = \frac{\omega_{eg} - \omega}{2} \quad (1.3.5)$$

The Rabi frequency describes the interaction's coupling strength that is given by:

$$\Omega = \frac{\vec{d}_{ge}.\vec{e}}{\hbar}\,\vec{E}(t). \tag{1.3.6}$$

We obtain the following coupled –the probability amplitudes' mode equations

$$\frac{d}{dt}\,C_e = \; -i\Delta C_e + i\frac{\Omega^*}{2}C_g \tag{1.3.7a}$$

$$\frac{d}{dt}\,C_g = \; +i\Delta C_g + i\frac{\Omega}{2}C_e. \tag{1.3.7b}$$

For the case of vanishing detuning it is especially easy to eliminate one of the variables and we arrive at

$$\frac{d^2}{dt^2}C_e = -\frac{|\Omega|^2}{4}C_e \tag{1.3.8a}$$

$$\frac{d^2}{dt^2}C_g = -\frac{|\Omega|^2}{4}C_g. \tag{1.3.8b}$$

The solution to this set of equations are the oscillations. If the atom is sometimes [14] $t = 0$ in the state of ground-, that is, $c_g(0) = 1$ while $c_e(0) = 0$, respectively, we arrive at

$$C_g(t) = \cos(\frac{|\Omega|}{2}t) \tag{1.3.9a}$$

$$C_e(t) = -i\sin(\frac{|\Omega|}{2}t). \tag{1.3.9b}$$

the probabilities for working out excited states or the atom in the ground are

$$\left|C_g(t)\right|^2 = \cos^2(\frac{|\Omega|}{2}t) \tag{1.3.10a}$$

$$|C_e(t)|^2 = \sin^2(\frac{|\Omega|}{2}t) \quad (1.3.10b)$$

This probability oscillates at the flopping frequency, which is reliant on frequency (that the detuning expresses) and the laser intensity (that the Rabi frequency expresses). However, these oscillations' amplitude, is solely reliant on the laser frequency, the maximum amplitude (probability) is one when the light is zero detuned, and the probability decreases when detuning increase, but there is always some possibility that at certain period, the atom is in the upper state. The absorption feature's variation [33] in the course of resonance as a resonance detuning's function; rate of ionization and Rabi frequency is theoretically simulated. It is displayed that at the inauguration of laser radiation, absorption introduces a two-level system's character. As the resonance detuning decreases, the absorption intensity increases and gets to a supreme peak when the detuning is equivalent to zero. A phenomenon that is very fascinating is going to be observed following a given time for laser radiation. Resonant absorption display itself as transparency. As the rate of ionization decreases, the transparent depth increases. This is accredited to the population evacuation in the state of excited resonant that decreases with the rate of ionization. In addition, it is discovered that with the frequency of Rabi increases, the resonant absorption at first increases before decreasing after getting to a supreme, absorption

transparency is going to emerge eventually. As Rabi frequency increases, the transparent width also increases. We understood these to the splitting of the level of energy (ac Stark effect) that the laser field induces. In a situation where the resonant absorption alters to the levels of splitting, transparency emerges at the original resonant point's position. The greater the frequency of Rabi is the wider the interval of the levels of splitting is going to be. As the Rabi frequency increases, the transparent width will as well increase.

1.4 Coherence Effects

Attracts coherent [35] between the levels of energy atomic system more consideration and plays a highly a prominent purpose in quantum physics. Where there are several impacts as a result of the atomic coherence, for instance EIT (electromagnetically induced transparency), EIA (electromagnetically induced absorption), amplification short of inversion and coherent population tapping, etc.

In addition, the atomic coherence has been applied in several applications, for example, the velocity chose coherent population trapping technique in light storage and sub-recoil laser cooling. In fact, majority of the experiments on EIA, AWI, CPT and EIT are carried out in room-temperature atomic vapor [37] the representative phenomena of the atomic coherence effect as a result of a multi-level atom interaction with two lasers are EIT (electromagnetically induced transparency) and

electromagnetically induced absorption.

1.4.1 Electromagnetically Induced Transparency (EIT)

It is [38] clear that in the atom-light interaction, nonlinear interference impacts could bring about important as well as main occurrences, [5-16-17-20-27] as such as transparency that electromagnetically induced it is means whereby a destructive quantum interference phenomena whereby optically thick medium become transparent in a narrow spectral range all over an absorption line. In addition, this transparency generates extreme dispersion" window" that brings about to "slow light".

Electromagnetically induced transparency can be occurs when the medium interacts with two laser fields of specific frequencies, a weak probe beam on a three level lambda Λ system and a strong control beam . All the atoms at two photon resonance are confined in a state of lower energy referred to as a dark state. The dark state does not consist of the excited state; therefore, probe beam does not further get absorbed. The transparency of the light is therefore the highest. This is referred to as Electromagnetically Induced, which could as well be applied electromagnetically induced transparency in several fields such as quantum information processing, quantum optics and nonlinear optics. The applications of electromagnetically induced transparency entail inducing of transparency in optically thick medium, which allows four wave mixing, creating alterations in the refractive index properties,

upholding slow light, enabling information storage as well as quantum computation. In order to have understanding of electromagnetically induced transparency we will be taken into account the 3-level lambda system that Fig. 2 illustrates with quantum lower states |1>, |2>, as well as an upper state |3>. A near-resonant light field consisting of two phase-coherent components of frequency the first the probe field is regulated to the resonance $\omega_p \approx \omega_{13}$and the second is the control field is regulated to the resonant frequency $\omega_c \approx \omega_{23}$. The laser field that drives the atomic [49] transition amid the upper state |1> and lower state |2> is pumping (or control laser) and the laser that drives transition between the states |1> and |3> is the probe lasers where an electron can transition between the states |1> and |3> also between the states |2> and |3> according to selection rules where the states |1> ↔|3> and [52] |2> ↔|3> are dipole-enabled transitions and state |1> ↔|2> is prohibited transitions

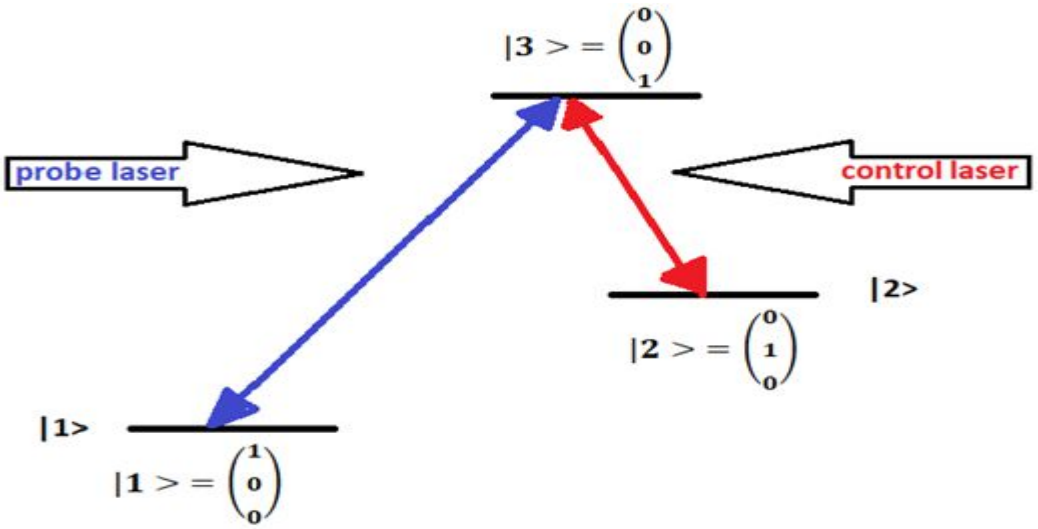

Figure2. Configuration for the interaction of three levels single lambda Λ system

The atomic free-evolution Hamiltonian $\hat{H}_A$ can therefore be expressed in this basis as a matrix with elements

$$\hat{H}_A = \begin{pmatrix} \hbar\omega_1 & 0 & 0 \\ 0 & \hbar\omega_2 & 0 \\ 0 & 0 & \hbar\omega_3 \end{pmatrix}. \quad (1.4.1.1)$$

Therefore we note this system will tend to settle in the lowest energy states |1> state due to spontaneous emission from higher energy states. The atom field interaction Hamiltonian $\hat{H}_{AF}$ can be write in the following

$$\hat{H}_{AF} = -\vec{E}\begin{pmatrix} 0 & 0 & \vec{d}_{13} \\ 0 & 0 & \vec{d}_{23} \\ \vec{d}_{31} & \vec{d}_{32} & 0 \end{pmatrix} \quad (1.4.1.2)$$

Note that many of the matrix elements of this Hamiltonian are zero. For example, the dipole elements $\vec{d}_{12}$ and $\vec{d}_{21}$ must be zero for the |1> →|2> transition to be dipole forbidden. Additionally, the diagonal terms must go to zero because of the spherical symmetry of the wave function. Additionally, the interaction term of the Hamiltonian it is useful to transform into the interaction picture of the unperturbed system. To do that, we use the time evolution operator as following

$$\hat{H}_{AF(RWA)} = -\vec{E}\begin{pmatrix} 0 & 0 & \vec{d}_{(13)}e^{-i\omega_{(13)}t} \\ 0 & 0 & \vec{d}_{(23)}e^{-i\omega_{(23)}t} \\ \vec{d}_{(31)}e^{i\omega_{(13)}t} & \vec{d}_{(32)}e^{i\omega_{(23)}t} & 0 \end{pmatrix} \quad (1.4.1.3)$$

whereas the electric field is a sum of cosines. These can be written instead as exponentials:

$$\vec{E}_{(t)} = \vec{E}_p \frac{1}{2}\left(e^{i\omega_p t} + e^{-i\omega_p t}\right) + \vec{E}_c \frac{1}{2}\left(e^{i\omega_c t} + e^{-i\omega_c t}\right) \qquad (1.4.1.4)$$

the nonzero elements become for the atom field collaboration

Hamiltonian under the turning wave approximation being:

$$\hat{H}_{AF\ (RWA)} = \frac{-1}{2}\begin{pmatrix} 0 & 0 & \vec{E}_p\vec{d}_{(13)}e^{-i\omega_p t} \\ 0 & 0 & \vec{E}_c\vec{d}_{(23)}e^{-i\omega_{(23)} t} \\ \vec{E}_p\vec{d}_{(31)}e^{i\omega_p t} & \vec{E}_c\vec{d}_{(32)}e^{i\omega_c t} & 0 \end{pmatrix}$$

(1.4.1.5)

The Rabi frequencies of this system are defined to be

$$\Omega_p = \frac{\vec{E}_p|\vec{d}_{13}|}{\hbar} \qquad (1.4.1.6a)$$

$$\Omega_c = \frac{\vec{E}_c|\vec{d}_{23}|}{\hbar} \qquad (1.4.1.6b)$$

The Hamiltonian atom- field interaction becomes

$$\hat{H}_{AF} = -\frac{\hbar}{2}(\Omega_p e^{-i\omega_p t}|1\rangle\langle 3| + \Omega_c e^{-i\omega_c t}|2\rangle\langle 3| + \Omega_p e^{i\omega_p t}|3\rangle\langle 1| +$$

$$\Omega_c e^{i\omega_p t}|3\rangle\langle 2|) \qquad (1.4.1.7)$$

In which Ω_p refers to the Rabi frequency corresponding to the probe field, whereas Ω_c refers to the Rabi frequency corresponding the control field.

We will write the atomic wave function as

$$\psi(t) = c_1(t)e^{-i\omega_1 t}\big|1> + c_2(t)e^{-i\omega_2 t}\big|2> + c_3(t)e^{-i\omega_3 t}|3> \quad (1.4.1.8)$$

We need to solve the time-dependent equation be using relation [14]

$$i\hbar\frac{d\Psi(t)}{dt} = \hat{H}\Psi(t) \qquad (1.4.1.9)$$

Which can be further solved such that there is a dark state, which is only

states' linear permutation |1> and |2> if the system is in what is known as the dark state which occur when the two photon detuning is equal zero:

$$|\mathrm{D}\rangle = \mathrm{c}_1(\mathrm{t})|1> -\mathrm{c}_2(\mathrm{t})|2> \quad (1.4.1.10a)$$

With coefficients given by

$$|\mathrm{D}\rangle = \frac{\Omega_\mathrm{c}}{\sqrt{\Omega_\mathrm{P}^2+\Omega_\mathrm{c}^2}}|1\rangle - \frac{\Omega_\mathrm{p}}{\sqrt{\Omega_\mathrm{P}^2+\Omega_\mathrm{c}^2}}|2\rangle \quad (1.4.1.10b)$$

This is a dark state, and we note that the dark state contains no components of |3> because it cannot absorb or emit any photons from the applied fields which results in the lack of absorption within the medium at the given frequencies because transitions to the |3> state are no longer allowed and thus energy cannot be absorbed from the photon.

1.4.2 Electromagnetically induced absorption (EIA)

EIA (Electromagnetically induced absorption) is opposite phenomenon of EIT in a sense that [39] in a situation where a sharp peak characterizes the absorption spectrum, this impact is named EIA (electromagnetically induced absorption) has been witnessed during the interaction of co-propagating, orthogonally polarized probe as well as pump beams with hyperfine transition[10-12].

However, in a closed system when the pump as well as probe beams have diverse polarizations, coherence transfer excite to electromagnetically induced absorption EIA.

Here EIA is correlated with creation of light induced Zeeman coherences

and their transfer to ground condition by impulsive discharge in the excited condition. This come about in the absence of ground state population trapping on the state angular moment of the excited condition is higher as compared to the one of ground condition and due to also [36] lasers duo two levels of degenerate atomic. Additionally, electromagnetically induced absorption can also arise when population transfer by collisions from the ground condition to an immediate level, which does not intermingle with the pump, is greater as compared to that from the excited condition. However electromagnetically induced absorption is observed in an open system, when the both of beams have same polarizations. It is important to note that electromagnetically induced absorption can only occur in the absence of population trapping and systems which behave as open Λ systems, which is not the same case to electromagnetically induced transparency. These systems can show both positive and negative dispersion. It is said be that absorption in these systems is reported have a peak at the line center accompanied with negative dispersion.

1.5 Four wave mixing in potassium mass number 39

The potassium isotope with mass number 39 has small hyperfine splitting compared to other alkali element. [1-2-3] It may behave qualitatively different in four waves mixing; this splitting is comparable to Doppler broadening. In the outermost shell, as an alkali atom, it has just one

electron while the core electrons protect the charge of the nucleus. As compared to the Doppler width of the optical transitions, the ground level frequency splitting is smaller and the spectrum of potassium is much less than those of any other alkali atom such as Na, Rb, and Cs, the hyperfine evolutions that start from a lone ground level are totally overlapped. Moreover, the components of hyperfine from the ground conditions levels could not be determined spectrally.

[44] FWM (Four-Wave Mixing) refers to a phenomenon third-order for non -linear process that syndicates three waves with the purpose of producing a fourth one, interaction of light and medium between electric field's four means, whereas these means are interacting with the medium [6]. All alkali atoms apart from Fr and Li so far were applied as gain medium for FWM.

FWM system comes from ability to generate quantum field correlations. Increased quantum correlations is present because non- linearity in such system is generated by coherence effect and "spontaneous free emission" rather than large populations of excited states and saturation.

[31] Diverse patterns have been applied in creation of paired photons, a point in case is atomic scheme usually employed in generating twin beams (higher gain of the probe and the conjugate beams) being off-resonant FWM in a scheme of dual lambda Λ, that check using D1 line of 39K. Therefore, [40] the conjugate and the gain of the probe is described

by using these relations $G_p=\frac{P_p}{P_{in}}$ and $G_c=\frac{P_c}{P_{in}}$, respectively, where P_p and P_c are the probe and conjugate's measured powers, in that order, and P_{in} is original power of the probe seed in the escalating medium.

In 39K, the D1 line is illustrated in figure.3, modeled as a four-level system that has a two hyperfine ground conditions levels and two levels of hyperfine excited. Generally, the excited state's hyperfine structure is hereby not taken into consideration, and it is taken to be a single level. Moreover, Fig4 illustrates the hyperfine levels' coupling of an alkali atom using a double lambda Λ scheme. Level |3> is $4P_{1/2}$, [31] whereas levels |1> and |2> refer to hyperfine levels of $4S_{1/2}$, F = 1 and F = 2, respectively.

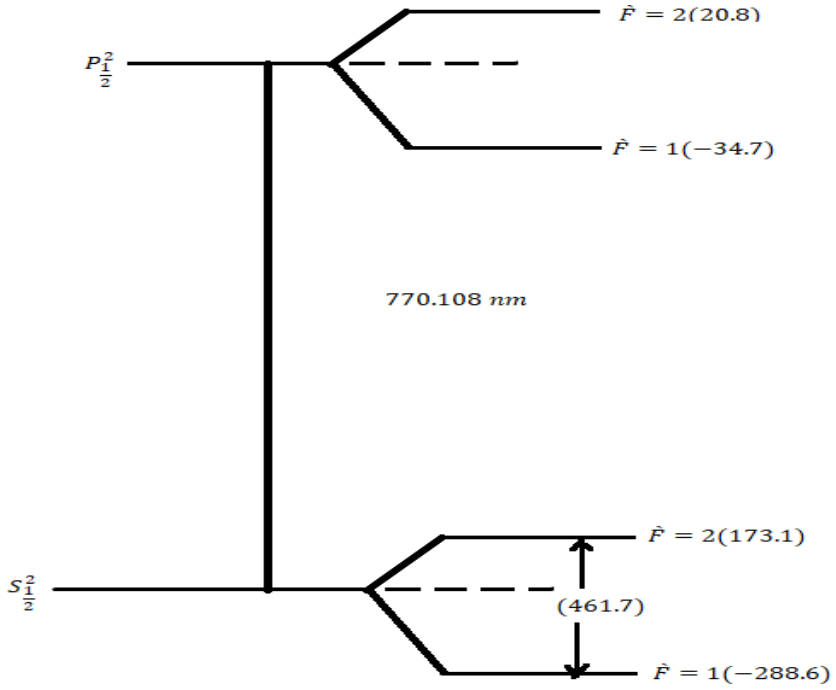

Figure 3: Optical of the [44] D1 –line's transitions of 39K

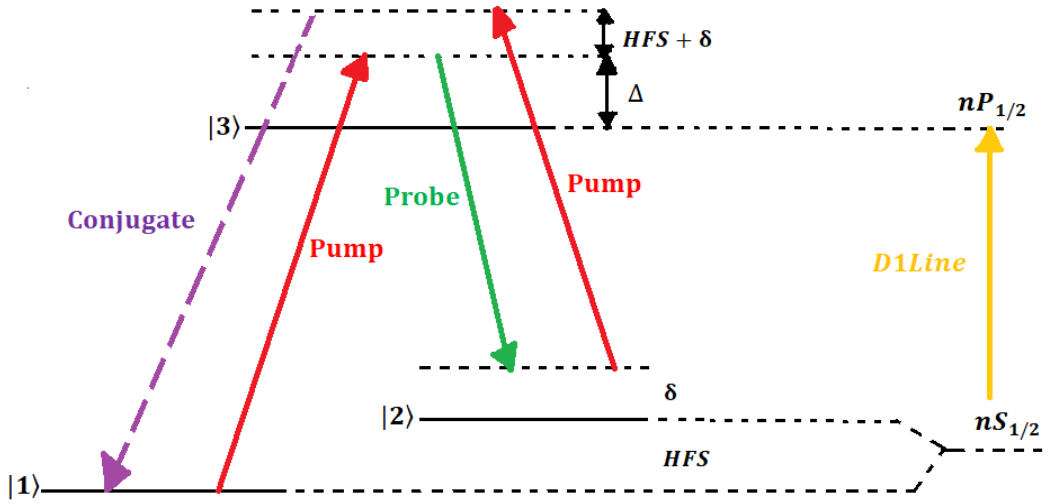

Figure 4. At D1 line, double Λ scheme of an alkali atom. HFS - hyperfine splitting, Δ - a photon detuning, δ - dual photon detuning. HFS of the nP1/2 (i.e.|3>) level is trivial than the ground condition HFS.

The initial Λ scheme comprises the strong pump, which pairs the lower sublevel of hyperfine |1> of the ground condition to the excited phase |3> with the a single photon detuning Δ of usually numerous hundred MHz .A different "leg" of the initial lambda Λ scheme is the feeble probe, which arouses the Stokes scattering from |3> to the sublevel of higher hyperfine |2> of the ground condition, with dual-photon detuning δ. The pump is adequately sturdy such that it is capable of driving the off-resonant transition commencing from |2>. Freshly generated conjugate closes the second Λ scheme via interesting anti-Stokes scattering to the lower sublevel hyperfine of this atomic scheme is that of an ordinary [31] EIT (electromagnetically induced transparency), and under particular circumstances, becomes FWM: by a proper choice of parameters. Whether system is going to behave as parametric amplifier or (EIT) is

reliant on laser detuning, primarily on pump power and atomic density. Large parametric gains were observed in alkali vapor in frequency region where concept of (EIT) is not valid or has negligible effect. Processes of resonant absorption in ordinary EIT result in large absorption and losses, and therefore probe gains >> 1 and generation of conjugate beam were observed in frequency region with large pump beam detuning and high atomic density.

1.6 Slow and Fast Light

With the use of material system, there is a possibility of exercising control of the propagation of light pulses' velocity. The slow and extremely propagation (which is slow as compared to the vacuum's light velocity) as well as fast propagation (that exceed the of light's vacuum velocity) have been witnessed. [4] To understand that, one must distinguish between light field's group velocity and the phase velocity. We note that the velocity with which a pulse of light propagates via a material system is provided by the group velocity. That one speaks of "fast" or "slow" light [28] depending the group velocity value ν_g as compared to the light velocity c in vacuum. Slow light is the condition $\nu_g \ll c$ and fast light is light traveling faster as compared to the light's speed in vacuum this could happen in a situation where $\nu_g > c$ or in a situation where ν_g is negative. This negative group velocity match up to

the situation where the pulse's peak transferred via an optical material appears prior to the incident light field's peak enters the medium. Generally, the transit time T through an optical medium could be exemplified as [30]

$$T = L/\nu_g \tag{1.6.1}$$

in which, L stands for the medium's physical length. When ν_g is negative therefore, the transit time via the medium will be negative as well.

We review the group and phase velocity's basic concepts as mentioned earlier. We start by taking into consideration a monochromatic plane wave of angular frequency ω that propagates via a refractive index' medium n this wave can be denoted by

$$\vec{E}(z,t) = Ae^{i(kz-\omega t)} + c.c. \tag{1.6.2}$$

In which $k = \frac{n\omega}{c}$

We describe the phase velocity ν_p to be the velocity whereby points of constant phase move via the medium. Because this wave's phase is denoted by

$$\varphi = kz - \omega t \tag{1.6.3}$$

Constant phase points move a distance Δz in a time Δt

$k\Delta z = \omega\Delta t$. Therefore $\nu_p = \Delta z/\Delta t$ or $\nu_p = \omega/k = c/n$.

In a situation where this pulse is to propagate short of distortion, the constituents with different angular frequency ω should travel with the

same phase velocity. For this to be expressed, thought arithmetically, we first write the wave's phase

$$\varphi = \frac{n\omega z}{c} - \omega t. \tag{1.6.4}$$

And require that there ought not be altered in φ to first order in

$$\omega \frac{dn}{d\omega}\frac{\omega z}{c} + \frac{nz}{c} - t = 0 \tag{1.6.5}$$

That could be written as $z = v_g t$ in which the group velocity is denoted by[29]

$$v_g = \frac{c}{n+\omega\frac{dn}{d\omega}} = d\omega/dk \tag{1.6.6a}$$

$$v_g = c/n_g \tag{1.6.6b}$$

Where the group index is

$$n_g = n + \omega\frac{dn}{d\omega}. \tag{1.6.7}$$

Note that if $\frac{dn}{d\omega}$ is non-zero, the group velocity can either increase or decrease. An increase in velocity yields fast light and a decrease yields slow light. Slow light is achieved in an EIT system (among other ways) through positive dispersion due to changes in the absorption. Fast light can be achieved by adding another laser field that excites another transition in the medium, creating what is known as a double Λ system. This system is characterized by negative dispersion, and therefore the medium has a group index less than one when excited by the probe and two control fields.

Chapter 2

2. Four Wave Mixing from density matrix element for conjugate

Maxwell's Equations describes an electromagnetic field's propagation that propagate an atomic vapor, [11] and these equations govern all of (classical) electricity and magnetism so, these four equations were collected by Maxwell and derived the form of the fields that satisfy them simultaneously in a number of simple circumstances. In rationalized MKS units, the following are differential forms of the equations:

$$\nabla \times \vec{E} = \frac{-\partial \vec{B}}{\partial t} \quad (2.1a)$$

$$\nabla \times \vec{H} = \vec{J}_f + \frac{\partial \vec{D}}{\partial t} \quad (2.1b)$$

$$\nabla . \vec{D} = \rho_f \quad (2.1.c)$$

$$\nabla . \vec{B} = 0 \quad (2.1.d)$$

With constitutive

$$\vec{D} = \epsilon_0 \vec{E} + \vec{P} \quad (2.2a)$$

$$\vec{B} = \mu_0 \left(\vec{H} + \vec{M}\right) \quad (2.2b)$$

At this juncture $\vec{D}$ is the displacement, $\vec{P}$ referring to the macroscopic polarization medium, $\overrightarrow{B}$ representing the magnetic induction, and $\vec{M}$ refers to the medium's magnetization.

The first one is Faraday's law of induction, while Ampere's law is the second one as Maxwell adjusted it to take account of the displacement

current $\partial \vec{D}/\partial t$ the fourth and third are Gauss 'laws for the magnetic and electric fields. The quantities $\vec{E}$ and $\vec{H}$ are the magnetic and electric field intensities. They are as well measured units of [ampere/m] and [volt/m] in that order. The quantities $\vec{B}$ and $\vec{D}$ are magnetic and electric flux densities. They are in units of [Weber/m^2, and [Coulomb/m2] or [Tesla]. $\vec{D}$ is as well referred to as the electric displacement, and $\vec{B}$ represents the magnetic induction. The quantities $\vec{J}$ and ρ are the electric current density and volume charge density (charge flux) of whichever external charges. Units of [Coulomb/m^3] and [Ampere/m^2] are what they are measured in. Presence of free charges in atomic vapor at temperatures of interest are negligible in gaseous phase for potassium atoms so, $\varrho_f = 0$ and $\vec{J}_f = 0$. Magnetic response of atoms is usually much smaller than their electric response below, $\vec{M} = 0$ therefore:

$$\nabla\vec{B} = 0, \nabla\vec{D} = 0 \tag{2.3}$$

we first derive wave equation for the vacuum. Given that the curl of Faraday's law both sides. We could apply the expression for the "Curl of the curl" to evaluate the curl of electric field's curl

$$\nabla \times \left(\nabla \times \vec{E}\right) = \nabla\left(\nabla.\vec{E}\right) - (\nabla.\nabla)\vec{E} \quad [14]$$

$$= \nabla\left(\nabla.\vec{E}\right) - \nabla.\nabla\vec{E}$$

$$= 0 - \nabla^2\vec{E} \quad [14] \tag{2.4}$$

given that $\nabla \times \vec{E} = \frac{-\partial \vec{B}}{\partial t}$ and $\nabla \times \vec{B} = \mu_0 \epsilon_0 \frac{\partial \vec{E}}{\partial t}$, that leads

$$\nabla \times \left(\nabla \times \vec{E}\right) = \frac{-\partial}{\partial t}\left(\nabla \times \vec{B}\right) \tag{2.5}$$

$$\frac{-\partial}{\partial t}\left(\mu_0 \epsilon_0 \frac{\partial \vec{E}}{\partial t}\right) = -\mu_0 \epsilon_0 \frac{\partial^2 \vec{E}}{\partial t^2} \tag{2.6}$$

Where $\nabla . \vec{E} = 0$

$$-\nabla^2 \vec{E} = -\mu_0 \epsilon_0 \frac{\partial^2 \vec{E}}{\partial t^2} \Rightarrow \frac{\partial^2 \vec{E}}{\partial t^2} = \frac{1}{\mu_0 \epsilon_0} \nabla^2 \vec{E}. \tag{2.7}$$

This expression recounts the electric field's temporal and spatial second derivatives and is referred to as the wave equation.

The speed is therefore:

$$c = \frac{1}{\sqrt{\mu_0 \epsilon_0}} \approx 3.10^8\, m/s.$$

It will be compensate for the velocity of light in the propagation equation we obtain

$$\nabla^2 \vec{E} = \frac{1}{C^2} \frac{\partial^2 \vec{E}}{\partial t^2} \tag{2.8}$$

The quantities $\epsilon_0$and μ_0 are the vacuum permittivity and permeability.

Similarly we derive wave equation for atomic vapor.

$$\nabla \times \left(\nabla \times \vec{E}\right) = \frac{-\partial}{\partial t}\left(\nabla \times \vec{B}\right) = -\mu_0 \frac{\partial}{\partial t} \nabla \times \vec{H} = -\mu_0 \frac{\partial}{\partial t}\left(\overrightarrow{J_f} + \frac{\partial \vec{D}}{\partial t}\right) \tag{2.9}$$

$$-\mu_0 \left(\frac{\partial}{\partial t} \sigma \vec{E} + \varepsilon_0 \frac{\partial^2 \vec{E}}{\partial t^2} + \frac{\partial^2 \vec{P}}{\partial t^2}\right) \tag{2.10}$$

$$\nabla \times \left(\nabla \times \vec{E}\right) + \mu_0 \sigma \frac{\partial \vec{E}}{\partial t} + \mu_0 \varepsilon_0 \frac{\partial^2 \vec{E}}{\partial^2} = -\mu_0 \frac{\partial^2 \vec{P}}{\partial^2 t} \tag{2.11}$$

$$-\nabla^2 \vec{E} + \mu_0 \sigma \frac{\partial \vec{E}}{\partial t} + \mu_0 \varepsilon_0 \frac{\partial^2 \vec{E}}{\partial t^2} = -\mu_0 \frac{\partial^2 \vec{P}}{\partial t^2} \tag{2.12}$$

Where, σ is conductivity. We will neglect the term with conductivity ($\sigma = 0$) since atomic gas is weakly ionized.

Assuming that the electromagnetic field is a plane wave that propagates along the z direction, we therefore disregard the dependence of x and y on $\vec{E}$. Therefore, $\nabla\vec{E} = 0$, then reduces to

$$-\nabla^2\vec{E} = \mu_0\epsilon_0\frac{\partial^2\vec{E}}{\partial t^2} - \mu_0\frac{\partial^2\vec{P}}{\partial t^2} \tag{2.13a}$$

$$\nabla^2\vec{E} - \mu_0\epsilon_0\frac{\partial^2\vec{E}}{\partial t^2} = \mu_0\frac{\partial^2\vec{P}}{\partial t^2} \tag{2.13b}$$

To compensate for the speed of light we get

$\nabla^2\vec{E} - \frac{1}{c^2}\frac{\partial^2\vec{E}}{\partial t^2} = \frac{1}{c^2\epsilon_0}\frac{\partial^2\vec{P}}{\partial t^2}$ therefore,

$$\left(\frac{\partial^2}{\partial z^2} - \frac{1}{c^2}\frac{\partial^2}{\partial^2 t}\right)\vec{E} = \frac{1}{c^2\epsilon_0}\frac{\partial^2\vec{P}}{\partial t^2} \tag{2.14}$$

Then the density matrix's elements $\hat{\varrho}$ are denoted by

$$\varrho_{nn} = \langle n|\hat{\varrho}|n\rangle \tag{2.15a}$$

$$\varrho_{nm} = \langle n|\hat{\varrho}|m\rangle \tag{2.15b}$$

The density operator's diagonal elements, $\varrho_{nn} = \langle n|n\rangle$ are named populations, and give the system's measurement probability in the state |n> similarly off-diagonal elements, $\varrho_{nm} = \langle m|n\rangle$ are referred to as coherences between states $|n\rangle$ and $|m\rangle$.

The atomic dipole, in the situation of an electric dipole changeover, could be written in the density matrix's system as

$$\langle \vec{d} \rangle = -e \sum_{n,m} \varrho_{n,m} \langle m|\vec{r}|n\rangle = \sum_{n,m} \varrho_{n,m} \vec{d}_{m,n} \quad (2.16)$$

we are aware that the sum is just the product's trace of the density and position operators. The electric field's propagation could be termed as

$$\left(\frac{\partial^2}{\partial z^2} - \frac{1}{c^2}\frac{\partial^2}{\partial^2 t}\right)\vec{E} = \frac{1}{c^2 \in_0}\frac{N}{V}\sum_{n,m} \vec{d}_{m,n}\frac{\partial^2}{\partial^2 t}\varrho_{n,m} \quad (2.17)$$

Where [43] N refers to the number of atoms and V stands for the volume while c is the light's speed. However, in a situation where the evolution could be designated in a Hamiltonian terms, it could therefore be revealed with ease that the following determines the evolution duration of the density matrix

$$\frac{\partial}{\partial t}\hat{\varrho}\,(t) = -\frac{i}{\hbar}\left[\hat{H}, \hat{\varrho}\,(t)\right] + \widehat{SE} + \hat{R}. \quad (2.18)$$

In which the Hamiltonian and the density operator are communicated by the term in square brackets [16], where $\hat{H}$ stands for the Hamiltonian that describes the atomic reaction to the electric field. And [31] $\widehat{SE}$ represents the impulsive discharge from the excited conditions, while $\hat{R}$ stands for the relaxation as a result of collisional dephasing and atom transit time induced loss that is equation called is the Optical Block Equation. It is expedient extracting the fast-oscillating time dependence of the electric field as well as the polarization with the use of the slowly-varying phase approximation and amplitude. An electric field that is almost-monochromatic could be parameterized as its polarization unit vector's

product, $\vec{e}$ as well as an envelope function, $\varepsilon(z,t)$

$\vec{E}(z,t) = \varepsilon(z,t)e^{ikz-i\omega t}\hat{\epsilon} + complexconjugate.$

In which ε is differs gradually in time t and z direction, in comparison with the optical frequency ω as well as the wave vector $k = \frac{\nu}{c}$:

$\frac{\partial\varepsilon}{\partial z} \ll k\varepsilon, \frac{\partial\varepsilon}{\partial t} \ll \omega\varepsilon.$

In the same way, the electric dipole moment's oscillation frequency is mainly determined by the electric field's frequency.

2.1. a Mathematical Formulation

For simplicity consider a two-level atomic system, so the excited levels and ground will be designated $|e\rangle$ and , $|g\rangle$ correspondingly, and the resonant frequency denoted by ω_0 (i.e., the splitting energy of the states' pair is $\hbar\omega_0$) and the transitions to other levels are negligible because of consider near-resonant interactions. Then the unperturbed atom's Hamiltonian can be written as:

$\hat{H}_0 = \hbar\omega_0|e\rangle\langle e|$ (2.1.a.1)

Suppose the atom is placed at $z = 0$ in an electric field of frequency ω, the field contains both positive- and negative-frequency modes in general given by:

$\vec{E}(z,t) = \vec{E}_0^{(+)}(z)e^{-i\omega t} + \vec{E}_0^{(-)}(z)e^{i\omega t}$ (2.1.a.2)

The overall Hamiltonian for the field and atom can be written as a summation of the atom–field interaction Hamiltonian $\hat{H}_{AF}$ and free

atomic Hamiltonian $\hat{H}_0$.

$$\hat{H} = \hat{H}_0 + \hat{H}_{AF} \quad (2.1.a.3)$$

Then under the dipole approximation the interaction Hamiltonian can be expressed as product of the electric field vector and the dipole moment as:

$$\hat{H}_{AF} = -\vec{d} \,.\, \vec{E} \quad (2.1.a.4)$$

Here, $\vec{d}$ is the atom's dipole moment operator. The atom does not have a dipole moment when it is in an energy eigenstate, so $\langle e|\vec{d}|e\rangle = \langle g|\vec{d}|g\rangle = 0$, mark the vanishing of diagonal matrix terms of $\vec{d}$. This means that defining $\vec{d}_{eg} = \langle e|\vec{d}|g\rangle$, that leads the off-diagonal matrix element are no vanishing.

Multiplying both sides of $\vec{d}$ we by the identity $\hat{I} = |e\rangle\langle e| + |g\rangle\langle g|$, we can write the dipole operator as:

$$\vec{d} = \langle g|\vec{d}|e\rangle(|g\rangle\langle e| + |e\rangle\langle g|). \quad (2.1.a.5)$$

The total atom–field Hamiltonian can thus be written as

$$\hat{H} = \hat{H}_0 + \hat{H}_{AF} = \hbar\omega_0|e\rangle\langle e| - \langle g|\vec{d}|e\rangle.\vec{E}\,(|g\rangle\langle e| + |e\rangle\langle g|). \quad (2.1.a.6)$$

Where the excited-state projection operator is denoted by $|e\rangle\langle e|$.

Moreover we can do the same for the dipole operator and analyze into rotating parts (both negative and positive)

$$\vec{d} = \langle g|\vec{d}|e\rangle(|g\rangle\langle e| + |e\rangle\langle g|)$$

$$= \vec{d}^{(+)} + \vec{d}^{(-)} \qquad (2.1.a.7)$$

Where $\vec{d}^{(+)}$ and $\vec{d}^{(-)}$ Compensation for the values of both dipole operator and electric field vector in equation for the atom–field interface Hamiltonian $\hat{H}_{AF}$ we get:

$$\hat{H}_{AF} = -\vec{d}\,.\,\vec{E}$$

$$= -\left(\langle e|\vec{d}|g\rangle|e\rangle\langle g| + \langle g|\vec{d}|e\rangle|g\rangle\langle e|\right).\left(\vec{E}_0^{(+)}(z)e^{-i\omega t} + \vec{E}_0^{(-)}(z)e^{i\omega t}\right)$$

$$= -(\vec{d}^{(+)}.\vec{E}_0^{(+)}(z)e^{-i\omega t} + \vec{d}^{(+)}.\vec{E}_0^{(-)}(z)e^{i\omega t})|e\rangle\langle g| - (\vec{d}^{(-)}.\vec{E}_0^{(+)}(z)e^{-i\omega t} + \vec{d}^{(-)}.\vec{E}_0^{(-)}(z)e^{i\omega t})|g><e| \qquad (2.1.a.8)$$

Recall the time requirements, $\vec{d}^{(\pm)} \sim e^{\mp i\omega_0 t}$, $\vec{E}^{(\pm)} \sim e^{\mp i\omega_0 t}$.

Through this equation it is clear that the first two elements rotate quickly while the last two elements (cross) rotate slowly that means that in the RWA (rotating-wave approximation) we only keep the slowly varying components in the interaction Hamiltonian to illustrate more, the laser field's detuning from the atomic resonance given by $\Delta = \omega - \omega_0$ so the terms in the Hamiltonians which oscillate with frequencies ($\omega + \omega_0$) are neglected due to fast oscillating terms while terms which oscillate with frequencies ($\omega - \omega_0$) are kept due to slow rotating elements. This calculation is called the RWA (Rotating Wave Approximation), where, ω represents the light frequency and ω_0 represents a transition frequency.

2.1. b The Rabi Frequency

The rate at which the population difference between the excited states and ground oscillates and is proportional to the EM field strength is called the Rabi frequency. Rabi frequency equals to frequency splitting of the optical field seeing in the relations of a monochromatic wave with a double level atom.

Definition

For simplicity we consider a two-level atom with an applied field in the rotating-wave approximation (RWA). Therefore the atom –field interaction Hamiltonian in the (RWA) is [15-13-18-19]

$$\hat{H}_{AF} = -\vec{d}\,.\vec{E} = -\vec{d}^{(+)}.\vec{E}^{(-)} - \vec{d}^{(-)}.\vec{E}^{(+)}. \qquad (2.1.b.1)$$

Using both equations for electric field and dipole operator in case dependence on the time. [38] In this picture, we can denote the atom-field Hamiltonian

$$\hat{H}_{AF} = -\langle g|\vec{d}|e\rangle\,(\vec{E}_0^{(-)}|g\rangle\langle e|\,e^{i\omega t} + \vec{E}_0^{(+)}|e\rangle\langle g|e^{-i\omega t})$$

$$= \frac{\hbar\Omega}{2}(|g\rangle\langle e|e^{i\omega t} + |e\rangle\langle g|e^{-i\omega t}) \qquad (2.1.b.2)$$

In this case, to find a Rabi frequency we have assumed that the electric field positive component is real

$$\Omega = -\frac{2\langle g|\vec{d}|e\rangle\,\vec{E}_0^{(+)}}{\hbar} = -\frac{\langle g|\vec{d}|e\rangle\vec{E}_0}{\hbar} \qquad (2.1.b.3)$$

2.2 The Maxwell Bloch Equations

While the Bloch equations define the change in the polarization of the

medium, the Maxwell equations define the change in the electric field. The two combined are called the Maxwell-Bloch equations [7- 8-13 -14-18]. Consider a two level system driven with Rabi frequency Ω. The density matrix, for two-level atom is

$$\varrho = \begin{pmatrix} \varrho_{gg} & \varrho_{ge} \\ \varrho_{eg} & \varrho_{ee} \end{pmatrix} \tag{2.2.1}$$

the square of a probability amplitude is the diagonal matrix elements, and coherences can be defined as the off-diagonal matrix elements. The density matrix for the pure state is as considered above.

$$\varrho = \begin{pmatrix} 1/2 & i/2 \\ -i/2 & 1/2 \end{pmatrix} \tag{2.2.2}$$

the coherences are not zero, and indeed. In defining the evolution in terms of a Hamiltonian, it can be definitely demonstrated that the density matrix of the time evolution is described by the following equation [15]:

$$\frac{d\varrho}{dt} = -\frac{i}{\hbar}\left[\hat{H}_A + \hat{H}_{AF}, \varrho\right]. \tag{2.2.3}$$

Where $\hat{H}_A$ the field- is free Hamiltonian and $\hat{H}_{AF}$ is the interaction Hamiltonian. However, the procedures that cannot be labeled based on a Hamiltonian can be included using density matrix formalism. This enables us to take in the impacts of spontaneous radiation. In an occasion that the $|e\rangle$ (excited state) decays at rate Γ, then the time evolution of the groups caused by spontaneous radiation, in this case ϱ_{gg} is

$$\frac{d\varrho_{ee}}{dt} = -\frac{d\varrho_{gg}}{dt} = -\Gamma\varrho_{ee}. \tag{2.2.4}$$

We note from the previous equation the impact of spontaneous radiation on the coherences is unclear

$$\frac{d\varrho_{eg}}{dt} = -\frac{\Gamma}{2}\varrho_{eg}, \quad \frac{d\varrho_{ge}}{dt} = -\frac{\Gamma}{2}\varrho_{ge} \tag{2.2.5}$$

The motion equation for the density matrix, comprising the Hamiltonian element caused by the contact with the exterior field and spontaneous radiation become of the form

$$\frac{d\varrho}{dt} = -\frac{i}{\hbar}[\hat{H}_A, \varrho] - \begin{pmatrix} -\Gamma\varrho_{ee} & \frac{\Gamma}{2}\varrho_{ge} \\ \frac{\Gamma}{2}\varrho_{eg} & \Gamma\varrho_{ee} \end{pmatrix} \tag{2.2.6}$$

Applying the time-independent state of the Hamiltonian

$$\hat{H} = \frac{\hbar}{2}\begin{pmatrix} 0 & \Omega \\ \Omega & -2\Delta \end{pmatrix} \tag{2.2.7}$$

Where, Δ is the one photon detuning and Ω represents the Rabi frequency. With matrix terms of the Hamiltonian, it is an possible to create the equations of motion for the matrix terms of the atomic density, then we obtain the set of equations

$$\dot{\tilde{\varrho}}_{gg} = \frac{i\Omega}{2}\left(\tilde{\varrho}_{ge} - \tilde{\varrho}_{eg}\right) + \Gamma\tilde{\varrho}_{ee} \tag{2.2.8a}$$

$$\dot{\tilde{\varrho}}_{ee} = -\frac{i\Omega}{2}\left(\tilde{\varrho}_{ge} - \tilde{\varrho}_{eg}\right) - \Gamma\tilde{\varrho}_{ee} \tag{2.2.8b}$$

$$\dot{\tilde{\varrho}}_{ge} = -\frac{i\Omega}{2}\left(\tilde{\varrho}_{ee} - \tilde{\varrho}_{gg}\right) - i\Delta\tilde{\varrho}_{ge} - \frac{\Gamma}{2}\,\tilde{\varrho}_{ge} \tag{2.2.8c}$$

$$\dot{\tilde{\varrho}}_{eg} = \frac{i\Omega}{2}\left(\tilde{\varrho}_{ee} - \tilde{\varrho}_{gg}\right) + i\Delta\tilde{\varrho}_{eg} - \frac{\Gamma}{2}\,\tilde{\varrho}_{eg} \tag{2.2.8d}$$

These equations (2. 2. 8abcd) are known as the optical Bloch equations

for a double-level atom and such equations define the free development of the double-level atom in the conventional monochromatic field.

2.2.1 Maxwell-Bloch equation for Double-Lambda system

We have a model consisting of four-level atom whose configuration is indicated in Figure 4. This scheme comprise four wave mixing [31] considered as atomic structure with two excited levels and two ground levels. We assume that the pump couples drives transitions between levels |1>and |3> and also between levels |2> and |4>. The probe couples also drives the |2> and |4> transition and conjugate couples drives by levels |1> and |4>. With these assumptions can be drive the total electric field is given by

$$\vec{E} = \sum_{i=d,p,c} \vec{e}_i \, E_i^{(+)} e^{-i\omega t + ik_i r} + c.c. \qquad (2.2.1.1)$$

Where the quantities $E_i^{(+)}$ are the gradually changing packets of the pump and probe and conjugate fields at positive frequencies.

Using Hamiltonian's total equation for the atom field system is denoted by

$$\hat{H} = \hat{H}_0 + \hat{H}_{AF} = \sum_{i=1}^{4} \hbar\omega_i \, |i><i| - \hat{d}.\vec{E}(r,t). \qquad (2.2.1.2)$$

Where the quantities $\hat{H}_0, \hat{H}_{AF}$ are the free atomic unperturbed Hamiltonian of the system, interaction Hamiltonian respectively. Also $\hbar\omega_i$ is the atom energy (where i is indicates pump or probe or conjugate frequency) and $\hat{d}$ is the moment of atomic dipole. The atomic dipole

moment has non-zero elements only for dipole allowed transitions

$$\hat{d} = \begin{pmatrix} 0 & 0 & \vec{d}_{(13)} & \vec{d}_{(14)} \\ 0 & 0 & \vec{d}_{(23)} & \vec{d}_{(24)} \\ \vec{d}_{(31)} & \vec{d}_{(32)} & 0 & 0 \\ \vec{d}_{(41)} & \vec{d}_{(42)} & 0 & 0 \end{pmatrix}$$

The Bloch equation for density matrix element has the ability to describe the atomic dynamics

$$\dot{\hat{\varrho}} = -\frac{i}{\hbar}\left[\hat{H} + \hat{\varrho}\right] + \widehat{SE} + \hat{R}, \qquad (2.2.1.3)$$

The quantity $\widehat{SE}$ stands for spontaneous radiation from the excited states, and $\hat{R}$ represents relaxation terms because collisional dephasing (time of the flight and dephasing) and atom transit time-based losses. The spontaneous emission cannot be formally incorporated in the atom Hamiltonian. It emerges with the interaction of the electromagnetic field treated quantum mechanically [22]. Full description starts with the composite system A+E where A stands for the atom and E for the environment which is EM field in our case. States are defined in a Hilbert space formed as a tensor product of Hilbert spaces for atom and environment. It evolves according to Schrodinger equation with Hamiltonian acting on composite Hilbert space. Since we are only interested in the state of the atom a partial trace over environment should be performed. General discussion of this problem leads to Lindblad equation [23]. Because partial trace leads to mixed states it is the equation

for the density matrix. It is different from Liouville-von Neumann equation for an additional term

$$\dot{\rho} = -\frac{i}{\hbar}[H, \rho] + \sum_i \Gamma_i (L_i \rho L_i^{\dagger} - \frac{1}{2} L_i^{\dagger} L_i \rho - \frac{1}{2} \rho L_i^{\dagger} L_i)$$

Here Γ_i are constants and L_i are operators which are non-hermitian. In our case the sum over i is the sum over allowed transitions so i ="1, 3", "1, 4", "2, 3", "2, 4" and Lindblad operators are given explicitly as

$$L_{1,3} = \begin{pmatrix} 0 & 0 & 1 & 0 \\ 0 & 0 & 0 & 0 \\ 0 & 0 & 0 & 0 \\ 0 & 0 & 0 & 0 \end{pmatrix}, L_{1,4} = \begin{pmatrix} 0 & 0 & 0 & 1 \\ 0 & 0 & 0 & 0 \\ 0 & 0 & 0 & 0 \\ 0 & 0 & 0 & 0 \end{pmatrix},$$

$$L_{2,3} = \begin{pmatrix} 0 & 0 & 0 & 0 \\ 0 & 0 & 1 & 0 \\ 0 & 0 & 0 & 0 \\ 0 & 0 & 0 & 0 \end{pmatrix}, L_{2,4} = \begin{pmatrix} 0 & 0 & 0 & 0 \\ 0 & 0 & 0 & 1 \\ 0 & 0 & 0 & 0 \\ 0 & 0 & 0 & 0 \end{pmatrix},$$

Then the spontaneous emission is determined by relation

$$\widehat{SE} =$$

$$\begin{pmatrix} \Gamma_{1,3}\varrho_{33} + \Gamma_{1,4}\varrho_{44} & 0 & -\frac{\Gamma_{1,3}+\Gamma_{2,3}}{2}\varrho_{13} & -\frac{\Gamma_{1,4}+\Gamma_{2,4}}{2}\varrho_{14} \\ 0 & \Gamma_{2,3}\rho_{33} + \Gamma_{2,4}\varrho_{44} & -\frac{\Gamma_{1,3}+\Gamma_{2,3}}{2}\varrho_{23} & -\frac{\Gamma_{1,4}+\Gamma_{2,4}}{2}\varrho_{24} \\ -\frac{\Gamma_{1,3}+\Gamma_{2,3}}{2}\varrho_{31} & -\frac{\Gamma_{1,3}+\Gamma_{2,3}}{2}\varrho_{32} & -\Gamma_{1,3}\rho_{33} + \Gamma_{2,3}\varrho_{33} & -\frac{\Gamma_{1,3}+\Gamma_{2,3}+\Gamma_{1,4}+\Gamma_{2,4}}{2}\varrho_{34} \\ -\frac{\Gamma_{1,4}+\Gamma_{2,4}}{2}\varrho_{41} & -\frac{\Gamma_{1,4}+\Gamma_{2,4}}{2}\varrho_{42} & -\frac{\Gamma_{1,3}+\Gamma_{2,3}+\Gamma_{1,4}+\Gamma_{2,4}}{2}\varrho_{43} & -\Gamma_{1,4}\varrho_{44} - \Gamma_{2,4}\varrho_{44} \end{pmatrix}$$

and the relaxation terms is [32]

$$\widehat{R} = -\gamma\left[\hat{\varrho} - \mathrm{diag}\left(\frac{1}{2}, \frac{1}{2}, 0, 0\right)\right] - \gamma_{\mathrm{deph}}[\hat{\varrho} - \mathrm{diag}(\varrho_{11}, \varrho_{22}, \varrho_{33}, \varrho_{44})].$$

(2.2.1.4)

Substituting the total Hamiltonian from (2.2.1.2) into equation (2.2.1.3) [31] gives rapid rotating terms in ϱ_{ij}, after substitution we get

$$\tilde{\varrho}_{ij} = e^{-i\omega_{(ij)}t+ik_{(ij)}r}\,\varrho_{ij}, \qquad (2.2.1.5)$$

Here, $\omega_{(ij)}$ are various angular frequencies

frequency for pump is $\omega_{(d)} = \omega_{(24)} = \omega_{(13)}$, and angular frequency for probe is $\omega_{(p)} = \omega_{(23)}$, while angular frequency for conjugate is $\omega_{(c)} = \omega_{(14)}$ and $\omega_{(12)} = \omega_{(13)} - \omega_{(23)}$ and $\omega_{(34)} = \omega_{(14)} - \omega_{(13)}$

Where $k_{(ij)}$ are wave vectors of calculations of wave vector

wave vector for pump is $k_{(d)} = k_{(24)} = k_{(13)}$, while wave vector for probe is $k_{(p)} = k_{(23)}$, also wave vectors of conjugate is $k_{(c)} = k_{(14)}$, $k_{(12)} = k_{(13)} - k_{(23)}$, $k_{(34)} = k_{(14)} - k_{(13)}$, With $k_{(c)} = 2k_{(d)} - k_{(p)} - \Delta k$,, where the geometric phase mismatch is Δk.

In the rotating wave approximation, oscillating elements with the total frequencies are ignored. One photon detuning can be defined as $\Delta_{(13)} = \Delta$, while two photon detuning as $\Delta_{(132)} = \delta$. The writing of medium's polarization can be in terms of the atomic eigenstate, so as to be in the form:

$$P = N\sum_{n,m} \vec{d}_{m,n}\,\varrho_{n,m} e^{-i\omega_{n,m}t}. \qquad (2.2.1.6)$$

Where, $\sum_{nm}$is the summation of the involved atomic transitions, $\vec{d}_{m,n}$ represents the dipole matrix term between n and m levels, $\varrho_{n,m}$stands for the density matrix term between n and m levels in a rotating structure,

and $\omega_{n,m}$ represents the frequency of the field that connects the transition between levels n and m.

Moreover, this can be solved using the last equation for polarization to write the propagation expressions for the gradually changing packets of the pump and probe and conjugate field on the z direction such equations are:

$$\left(\frac{\partial}{\partial z}+\frac{1}{c}\frac{\partial}{\partial t}\right)E_d^{(+)}=i\,\frac{kN}{2\mathscr{E}_0}d\left(\tilde{\varrho}_{(42)}+\tilde{\varrho}_{(31)}\right), \tag{2.2.1.7a}$$

$$\left(\frac{\partial}{\partial z}+\frac{1}{c}\frac{\partial}{\partial t}\right)E_p^{(+)}=i\,\frac{kN}{2\mathscr{E}_0}d\tilde{\varrho}_{(32),} \tag{2.2.1.7b}$$

$$\left(\frac{\partial}{\partial z}+\frac{1}{c}\frac{\partial}{\partial t}\right)E_c^{(+)}=i\,\frac{kN}{2\mathscr{E}_0}d\tilde{\varrho}_{(41),} \tag{2.2.1.7c}$$

Here, N is the atom density, c is the speed of light, while k represents the wave vector.

From above relations finally we can write the optical Bloch equation for double lambda system [25]

$$\dot{\hat{\varrho}}_{11}=\gamma\left(\frac{1}{2}-\varrho_{11}\right)+\Gamma_{1,3}\varrho_{33}+\Gamma_{1,4}\varrho_{44}+\frac{i}{\hbar}\left(E_d^{(+)^*}d\varrho_{31}-E_d^{(+)}d\varrho_{13}+E_c^{(+)^*}d\varrho_{41}-E_c^{(+)}d\varrho_{14}\right),$$

$$\dot{\hat{\varrho}}_{22}=\gamma\left(\frac{1}{2}-\varrho_{22}\right)+\Gamma_{2,3}\varrho_{33}+\Gamma_{2,4}\varrho_{44}+\frac{i}{\hbar}\left(E_p^{(+)^*}d\varrho_{32}-E_p^{(+)}d\varrho_{23}+E_d^{(+)^*}d\varrho_{42}-E_d^{(+)}d\varrho_{24}\right),$$

$$\dot{\hat{\varrho}}_{33}=-\varrho_{33}\gamma-\Gamma_3\varrho_{33}+\frac{i}{\hbar}\left(E_d^{(+)}d\varrho_{13}-E_d^{(+)^*}d\varrho_{31}+E_p^{(+)}d\varrho_{23}-E_p^{(+)^*}d\varrho_{32}\right)$$

$$\dot{\varrho}_{12} = -\left(\gamma + \gamma_{deph} + i\Delta_{132}\right)\varrho_{12} + \frac{i}{\hbar}\left(E_d^{(+)^*} d\varrho_{32} - e^{izΔk} E_d^{(+)} d\varrho_{14} + e^{izΔk} E_c^{(+)^*} d\varrho_{42} - E_p^{(+)} d\varrho_{13}\right)$$

$$\dot{\varrho}_{13} = -\left(\gamma + \gamma_{deph} + \frac{\Gamma_3}{2} + i\Delta_{13}\right)\varrho_{13} + \frac{i}{\hbar}\left(E_d^{(+)^*} d\varrho_{33} - E_d^{(+)^*} d\varrho_{11} + E_c^{(+)^*} d\varrho_{43} - E_p^{(+)^*} d\varrho_{12}\right)$$

$$\dot{\varrho}_{14} =$$

$$-\left(\gamma + \gamma_{deph} + \frac{\Gamma_4}{2} + i\Delta_{1324}\right)\varrho_{14} + \frac{i}{\hbar}\left(E_d^{(+)^*} d\varrho_{34} - e^{-izΔk} E_d^{(+)^*} d\varrho_{12} + E_c^{(+)^*} d\varrho_{44} - E_c^{(+)^*} d\varrho_{11}\right),$$

$$\dot{\varrho}_{23} = -\left(\gamma + \gamma_{deph} + \frac{\Gamma_3}{2} + i\Delta_{13}\right)\varrho_{23} + \frac{i}{\hbar}\left(E_p^{(+)^*} d\varrho_{33} - E_d^{(+)^*} d\varrho_{21} + e^{-izΔk} E_d^{(+)^*} d\varrho_{43} - E_p^{(+)^*} d\varrho_{22}\right),$$

$$\dot{\varrho}_{24} = -\left(\gamma + \gamma_{deph} + \frac{\Gamma_4}{2} + i\Delta_{1324}\right)\varrho_{24} + \frac{i}{\hbar}\left(E_d^{(+)^*} d\varrho_{44} - E_d^{(+)^*} d\varrho_{22} + e^{izΔk} E_p^{(+)^*} d\varrho_{34} - e^{izΔk} E_c^{(+)^*} d\varrho_{21}\right),$$

$$\dot{\varrho}_{34} = -\left(\gamma + \gamma_{deph} + \frac{\Gamma_3}{2} + \frac{\Gamma_4}{2} + i\Delta_{1324} - i\Delta_{13}\right)\varrho_{34} + \frac{i}{\hbar}\left(E_d^{(+)} d\varrho_{14} - e^{-izΔk} E_d^{(+)^*} d\varrho_{32} + e^{-izΔk} E_p^{(+)} d\varrho_{24} - E_c^{(+)^*} d\varrho_{31}\right)$$

Here, $E_d^{(+)}$, $E_p^{(+)}$, $E_c^{(+)}$ represents field amplitude of positive rotating components for the probe, pump, and the combination, respective.

γ is the relaxation rate, Δk is the phase divergence described as $\Delta k = 2k_d - k_p - k_c$, where k_d, k_p, k_c are the pump and probe and

conjugate wave vectors respectively, where γ_{deph} is the dephasing decay rate, [46] Δ_{13} is one photon detuning, Δ_{132} is two photon detuning, Δ_{1324} is the [31] overall level |4> detuning defined as

$$\Delta_{1324} = \left(2\omega_d - \omega_p\right) - (\omega_4 - \omega_1),$$

where $\Gamma_{i,j}$ is the population rate of decay from level j to level i. When deriving such equations, it was supposed that the overall rate of decay of the excited states are the equal and have comparable branching proportions to the two grounds states, i.e., $\Gamma_4 = \Gamma_{1,4} + \Gamma_{2,4}$ and $\Gamma_3 = \Gamma_{1,3} + \Gamma_{2,3}$, this leads to $\Gamma_4 = \Gamma_3 \equiv \gamma$ and$\Gamma_{1,4} = \Gamma_{2,4} = \Gamma_{1,3} = \gamma/2$.

Chapter 3

3. Important Quantities

3.1 Speed of light and Group Velocity

The symbol c represents the velocity of propagation of electromagnetic waves including light waves, which is comparable to the speed of light in a vacuum (free space). This symbol is therefore an important physical constant. The light velocity in a vacuum plays a fundamental role in current physics as c is the reference speeds of transmission of all physical phenomena and is constant, i.e., is unchangeable under a transfer from one reference point to the other. A signal can only be sent at the speed c in a free space, but no signal can be sent at greater speeds than$c$. Therefore the speed of all electromagnetic radiation in vacuum is the same, approximately 3×10^8 meters per second. Usually, light cannot be transmitted at a speed equal to c in a medium. Different forms of light wave will always propagate at various speeds, for instance the speed of light in a clear medium is usually below the speed, c, in a free space. Refractive index (n) of the medium refers to the ratio of the speed in a free space to the speed in the material defined as

$$n = c/v_p \tag{3.1}$$

the symbol, n, is always greater than 1since the speed of light is highest in vacuum.

Now the phase velocity for an electromagnetic wave of angular frequency

ω is given by

$$v_p = \omega/k \tag{3.2}$$

where wave vector symbol is k .

Whereas the velocity's of group the velocity with that wave packet obtained due to superposition of wave traveling in a group is famously known as group velocity and denoted by is v_g

$$v_g = d\,\omega/dk \tag{3.3}$$

It is known that k for the value of $\omega = kc/n$ we get [19]

$$\frac{1}{v_g} = \frac{dk}{d\omega} = \frac{d}{d\omega}\left(\frac{n\omega}{c}\right) \tag{3.4a}$$

$$\frac{1}{v_g} = \frac{1}{c}\left(n + \omega\frac{dn}{d\omega}\right) \tag{3.4b}$$

$$v_g = \frac{c}{\left(n+\frac{d\omega}{dn}\right)} \tag{3.5}$$

3.2 Full width at Half maximum

FWHM (Full width at half maximum) is a variable applied in describing the measurement of a peaked function or curve [21]. It is denoted by the space between two points on the curve where the function attains half its peak value and the horizontal separation between the two points is referred to as the FWHM.

FWHM is applied to such phenomena as the sources' spectral width used for optical communications as well as important measure of the quality of an imaging device and its spatial resolution.

Can be obtaining the full measurement of the Gaussian curve at half the maximum as follows:

$$f(x) = Ae^{\frac{-(x-x_0)^2}{\sigma^2}} \quad (3.2.1)$$

The parameter A is the height of the curve's peak, σ represent the standard deviation, and x_0 represents the estimated figure.

Then we can derive the correlation between the standard deviation and FWHM as follows:

$$\frac{1}{2} = exp\left[\frac{-(x-x_0)^2}{\sigma^2}\right] \quad (3.2.2a)$$

$$\frac{(x-x_0)^2}{\sigma^2} = ln2 \quad (3.2.2b)$$

$$(x - x_0)^2 = \sigma^2 ln2 \quad (3.2.2c)$$

$$x_{1,2} = x_0 \pm \sigma\sqrt{ln2} \quad (3.2.2d)$$

$$x_2 - x_1 \equiv FWHM = 2\sigma\sqrt{ln2} \quad (3.2.2e)$$

$$FWHM = \left[2\sqrt{ln2}\right]\sigma \quad (3.2.3)$$

Note that in the previous relation, the width is not related to the estimated value x_0.

3.3 GAIN

The gain also called the amplification factor, it known is the extent to which a device boosts the strength of a signal, it's symbolized by G. [1-25] Therefore the gain from the four wave mixing (FWM) process, is measured experimentally as followings

$$G = \frac{P_{\grave{P}}}{P_P} \quad (3.3.1)$$

Where the power of the output beam is denoted by $P_{\grave{P}}$ and the power of an input probe is P_P. The output gain is determined by a number of factors, such as the input angle of the seed, the two photon detuning δ and one photon detuning Δ, the intensity of the pump, and the cell temperature.

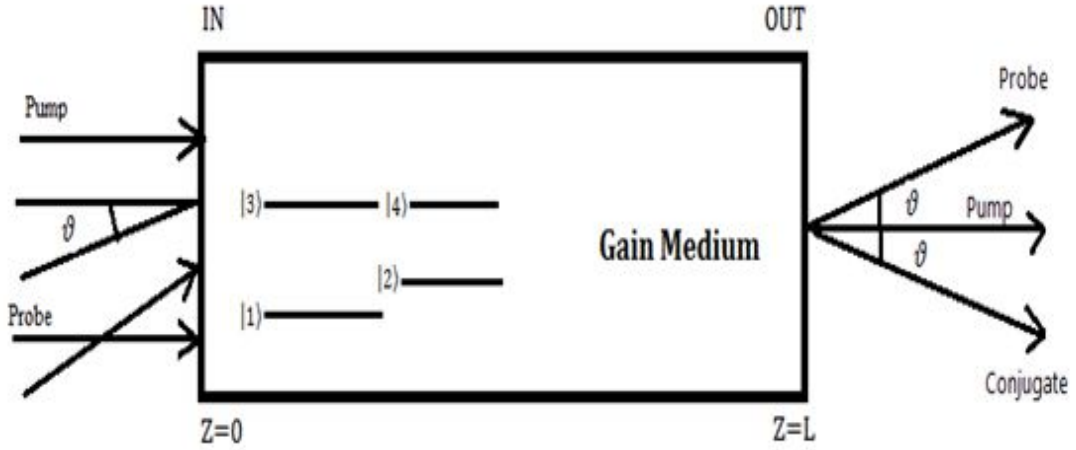

Fig5. Scheme of Potassium Cell and input and output fields

Fig. 5 demonstrate the gain for the probe as well the conjugate fields using the ratio between input probe power and output field power.

$$G = P_{out}/P_{in} \quad (3.3.2)$$

where P_{out} represent the output power and P_{in} is the input power of a CW input signal. From this relationship can be inferred the gain for probe beam following as

$$G_P = \frac{P_P^{max}(Z=L)}{P_P^{max}(Z=0)} = \frac{|\varepsilon_P^{max}(Z=L)|^2}{|\varepsilon_P^{max}(Z=0)|^2} \quad (3.3.3)$$

Similarly it will be Use same as relationship to find the gain for conjugate

beam

$$G_c = \frac{P_c^{max}(Z=L)}{P_P^{max}(Z=0)} = \frac{|\varepsilon_c^{max}(Z=L)|^2}{|\varepsilon_P^{max}(Z=0)|^2} \quad (3.3.4)$$

Where P_P is the probe power and P_c is the conjugate power

3.4 Continuous Wave Results

The gains of two beams (probe and conjugate) in this section was presented as a function of one of four wave mixing parameters, two-photon detuning, one photon detuning, gas density, and angle between probe and pump. We will show the dependence on any of this parameter depends, sometimes vary strongly, on values of other parameters. We present comparison between thin cell 1 cm and thick cell 4cm.

3.4.1 Thin and Thick cell, Strong Pump Intensity

We present in [31] this aspect the results we got with these common parameters: propagation distance zmax = 1cm or 4cm, electric field amplitude of the pump $E_d^{(+)} = 9800\frac{N}{C}$, that corresponds to Rabi frequency Omega $\Omega_d = 3.23$GHz and electric field amplitude of the probe $E_P^{(+)} = 71.9\ \frac{N}{C}$, that corresponds to Rabi frequency Omega $\Omega_P = 22.6$ MHz, electric field amplitude of the conjugate is $E_c^{(+)} = 1$, that corresponds to Rabi frequency Omega $\Omega_c = 330$ KHz, gamma $= 10^5$ MHz and depasing rate = 0, atom density is $Nc = 1 * 10^{18}cm^{-3}$, one-photon detuning is $\Delta = 2 * pi * 1 * 10^9$ GHz, anglels between pump

and probe and pump and conjugate $\vartheta = 7.5$ mrad, two photon detuning for thin cell 1 cm and thick cell 4cm are: $\delta = -1.10 * 10^8$MHz, $\delta = -0.80 * 10^8$MHz. Electric field amplitude of the conjugate at $z = 0$ is taken to be 1 because numerical instabilities may occur if initial value was 0 in the code.

3.4.1. a Adopt the gain on the angle between the pump and probe

FWM phase matching produces conjugate and probe gains in terms of the angle between the probe and the pump. Fig.6 present calculated conjugate and probe beam gains in terms of the angle ϑ. Depending on values of some factors, phase matching condition is met at various angles ϑ. The gain for longer cell is higher than the gain for shorter cell, as expected, but also the peak is narrower, and density greater. From the figures, FWM gains happen in a small range of angles, where the biggest is away from zero. This is due to the phase mismatch. Three coherent electromagnetic fields are propagating through the medium. But each of them have its own refractive index. So wavelengths are compressed by different factors. The consequence is that, for propagating waves, the phase mismatch will build across the cell. If the parameters are correctly set to cause FWM at the entrance of the cell, then after a while phases of the waves will be out of synchronization and so the process of four-wave

mixing will not extend and only absorption will happened. We see this as a very low gain at $\vartheta = 0$ in this graphs suppose now that an [50] angle exists between probe and the pump. By projecting the two lasers' waves on the propagating direction their wavelengths will be compressed differently, so this added shrinking of wavelength may compensate for different compression of wavelengths caused by different refractive indexes. From the graphs we see that at around $\vartheta = 7\text{mrad}$ phase matching condition $\vec{k}_d + \vec{k}_d = n_p\vec{k}_p + \vec{k}_c$ is restored. In such equation it is used the fact that n_d and n_c are approximately equal to 1.

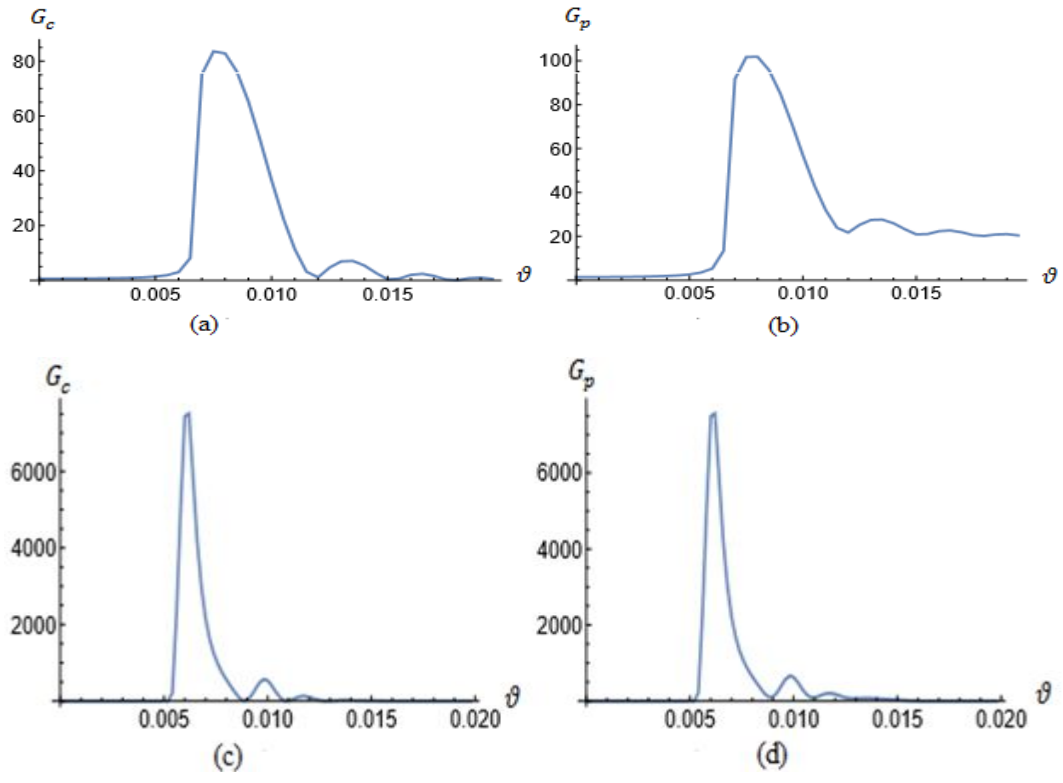

FIG.6. The conjugate and probe beams' calculated gain in terms of the angleϑ, for one pump power, $\Omega = 3.23GHz$, $Nc = 1 * 10^{18}cm^{-3}$. For 1cm cell (a, b). $\delta = -1.10 * 10^{8}MHz, \Delta = 1GHz, \vartheta = 7.5mrad$. For 4cm cell (c, d). $\delta = -0.80 * 10^{8}MHz, \Delta = 1GHz, \vartheta = 6mrad$

3.4.1.b Dependence on one – photon detuning

Calculated conjugate and probe beam gains [48] in terms of one – photon detuning in Fig. 7, [31] potassium possesses much bigger Doppler widening than any other alkali, of the order of 1GHz. The extents of Δ for big gains of FWM system that uses double Λ scheme is determined by the width of Doppler line widening in hot alkali fumes. The gain for longer cell is higher than the gain for shorter cell also the peak is wider see figures. The dependence on one-photon detuning exposes the difference between one-photon and two-photon resonances. One of the conditions for FWM is that two-photon detuning is in the MHz range, so it is near resonant. One may expect a monotonously decreasing dependence of four-wave mixing on one-photon detuning. But that is not the case. At low OPD there is a parasitic effect that restrict the gain in the medium. It is simply one-photon absorption of the pump photons. There is a competition of this two effects. One-photon absorption inhibits the gain while two-photon absorption created four-wave mixing. For small OPD former affects the final result, while for higher FWM is uninhibited. Of course for too big one-photon detunings there is not enough power in the pump laser to drive two-photon transitions so gain tend to zero.

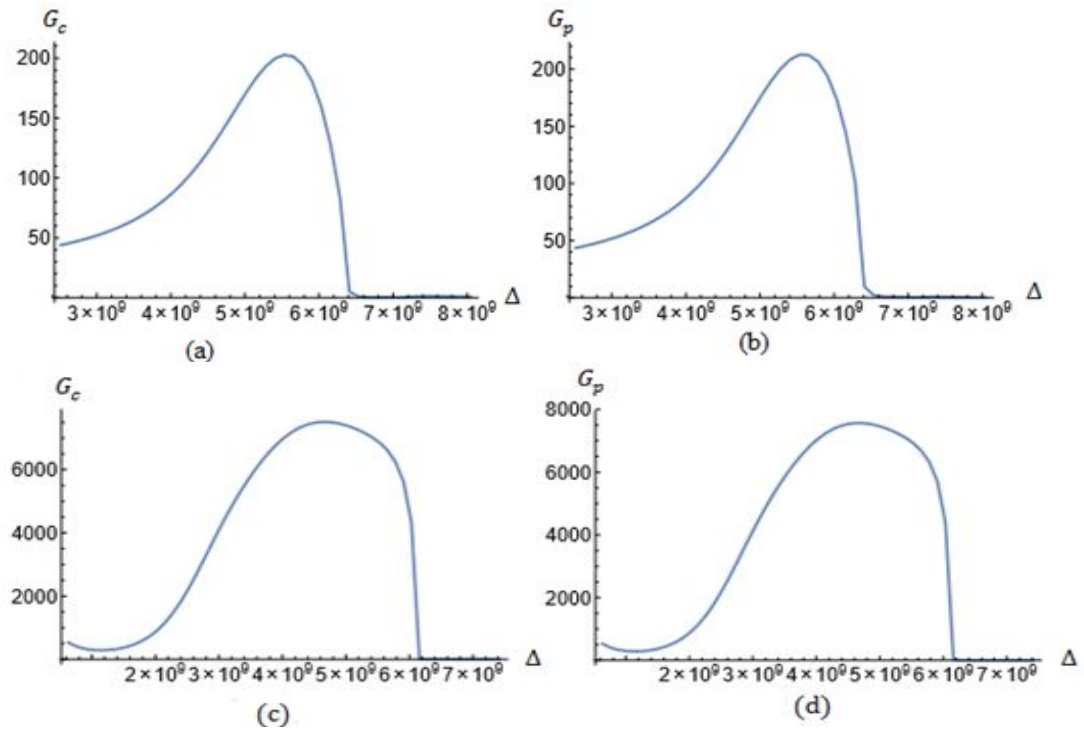

FIG.7. The conjugate and probe beams' Calculated gain as a function of Δ, for one pump power, $\Omega = 3.23GHz$, $Nc = 1 * 10^{18}cm^{-3}$. For 1cm cell (a, b), $\delta = -1.10 * 10^8 MHz$, Δ= $1GHz, \vartheta = 7.5mrad$. For 4cm cell (c, d), $\delta = -0.80 * 10^8 MHz$, Δ= $1GHz, \vartheta = 6m$

3.4.1.c Dependence on two - photon detuning

Fig.8 presents the dependence of twin beams' gains as a function of δ. The Figure contains results that show that gain maximums, at maximum two photon detuning δm, are [31] move from two photon resonance (δ ≈ 0). Such a transfer is primarily due to the differential Stark move smallest two photon detuning δs, of two ground state hyperfine structure because of different detuning from the non-resonant pump. Maximum two photon detuning δm moves to larger δ as one photon detuning Δ increases. Maximum of gains are depending on Δ and potassium density and for all other parameters fixed, it is more negative if Δ is smaller. The gain for

longer cell is higher than the shorter cell also the peak is wider. As a nonlinear process FWM relies on two-photon resonance. In the similar manner as one-photon detuning causes drop in one-photon absorption the two-photon detuning decreases gain of FWM. Displacement of the maxima in Fig. 8. May be attributed to AC Stark shift because there is a powerful drive laser.

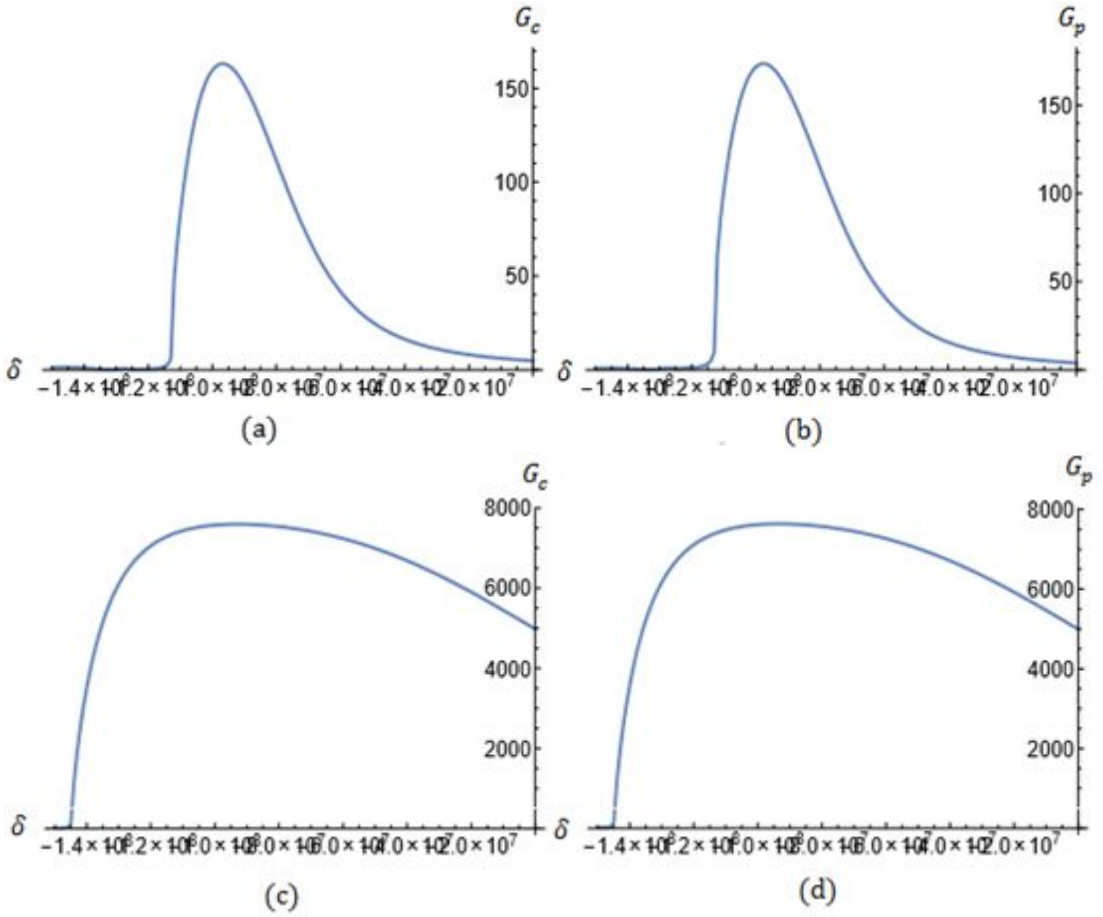

FIG.8. Conjugate and probe beams' calculated gain of the in terms of δ, for one pump power, $\Omega = 3.23GHz$, $Nc = 1 * 10^{18}cm^{-3}$. For 1cm cell (a, b). $\delta = -1.10 * 10^{8}MHz, \Delta = 1GHz, \vartheta = 7.5mrad$. For 4cm cell (c,d). $\delta = -0.80 * 10^{8}MHz, \Delta = 1GHz, \vartheta = 6mrad$

3.4.2 Thin and Thick cell, Medium Pump Intensity

The results of twin beams' gains are present with these common

parameters:

propagation distance zmax = 1cm or = 4cm, electric field amplitude of the pump $E_d^{(+)} = 6000 \frac{N}{C}$, that corresponds to Rabi frequency Omega $\Omega_d = 1.94$ GHz and electric field amplitude of the probe $E_P^{(+)} = 71.9 \frac{N}{C}$, that corresponds to Rabi frequency Qmega $\Omega_P = 22.6$ MHz, electric field amplitude of the conjugate is $E_c^{(+)} = 1$, that corresponds to Rabi frequency Omega $\Omega_c = 330$ KHz, gamma $= 10^5$ MHz and depasing rate $= 0$, atom density is $Nc = 1 * 10^{18} cm^{-3}$. One-photon detuning is $\Delta = 2 * pi * 1 * 10^9$ GHz, anglels between pump and probe and pump and conjugate $\vartheta = 2.8$ mrad, two photon detuning for propagation distance zmax = 1cm and = 4cm respectively. Are $\delta = -0.90 * 10^8$ MHz, $\delta = -0.60 * 10^8$ MHz.

3.4.2. a Dependence of gain on angle θ

Graphs in Fig. 9 are obtained for one pump Rabi frequency. From the results, the FWM's gains are quite different at lower Rabi frequencies, at lower density and power. FWM phase matching occur at smaller angles, since gain is inversely proportional to ϑ. The gain for longer cell is higher and peak is wider than the gain for shorter cell. The difference between Fig 6. And Fig 9. is that now with lower pump intensity the phase shifts are not so prominent so for a short cell the maximum of the gain is at

$\vartheta = 0$. In other words propagation distance is not long enough for a phase mismatch to accumulate. There is a negative impact of phase mismatch as it can be seen from Figs. 9c, d where the maximum of the gain is for positive angles ϑ.

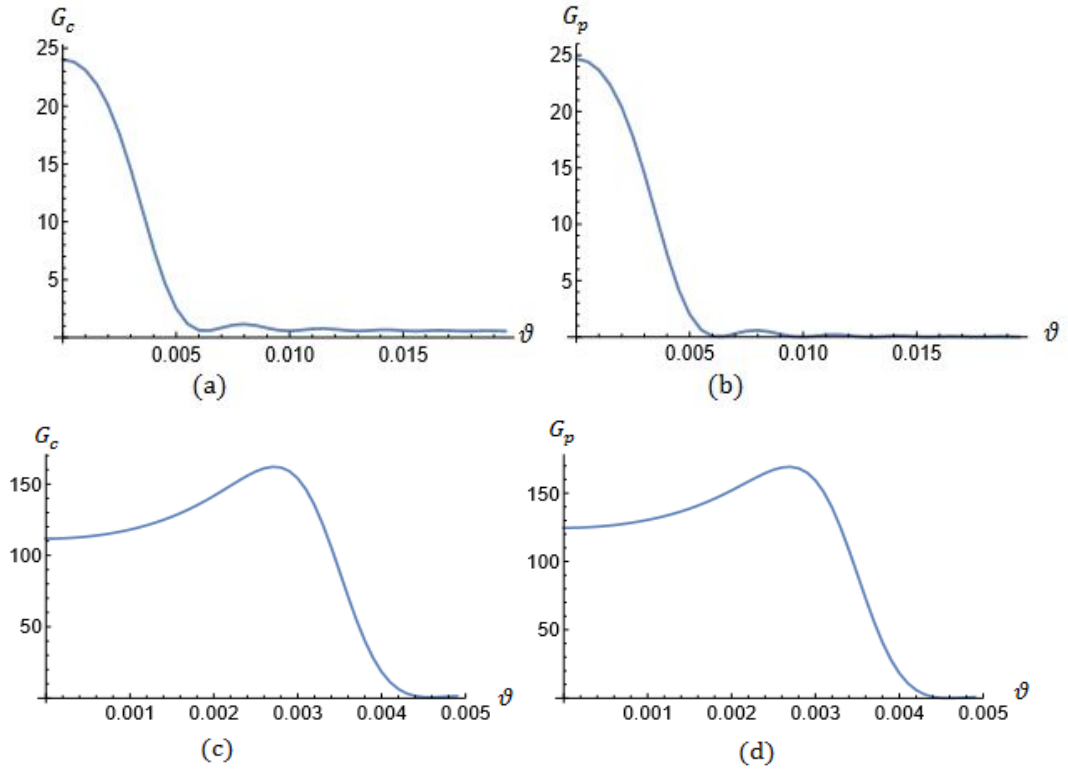

FIG.9. Calculated effects of pump power on conjugate and probe beams as a function of angle ϑ, $\Omega = 1.94$ GHz, $Nc = 1 * 10^{18}\text{cm}^{-3}$. For 1cm cell (a, b). $\delta = -0.60 * 10^{8}$, $\Delta =$ 1GHz, $\vartheta = 2.8$ mrad. For 4cm cell (c, d). $\delta = -0.90 * 10^{8}$, $\Delta =$ 1GHz, $\vartheta = 2.8$ mrad

3.4.2. b Dependence on one -photon detuning

Calculated of gains as a function of one-photon resonance Δ are given in Fig10. One-photon detuning for maximum gains, maximuma one photon detuning Δm, are close to 1GHz, but this value moves around depending on the value of δ. For the same angle θ, the maximum one photon

detuning Δm will move to different value when two photon detuning δ is changed, and the width in the lift curve is widder than the right curve. The gain for longer cell is higher also the peak is wider than the shorter cell.

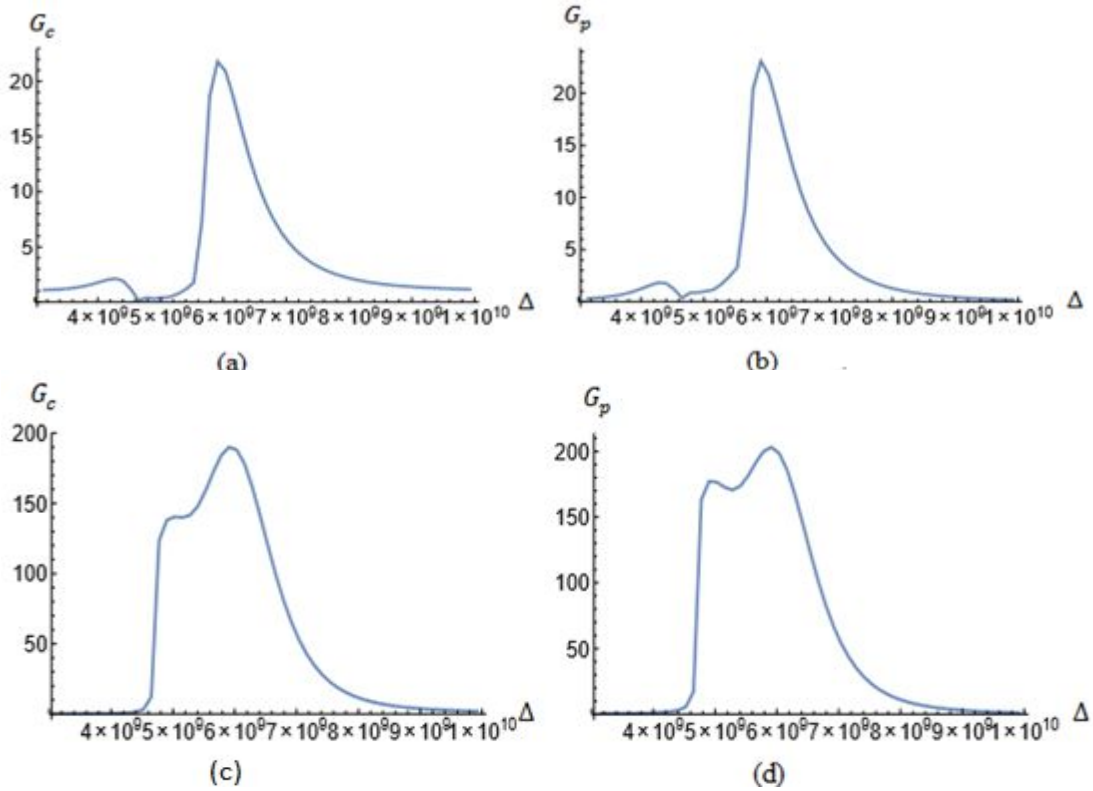

FIG.10. Calculated effects of pump power on conjugate and probe beams as a function of one photon detuning Δ, $\Omega = 1.94$ GHz , $Nc = 1 * 10^{18}\text{cm}^{-3}$.

For 1cm cell (a, b). $\delta = -0.60 * 10^{8}$, $\Delta = 1\text{GHz}, \vartheta = 2.8$ mrad.

For 4cm cell (c, d). $\delta = -0.90 * 10^{8}$, $\Delta = 1\text{GHz}, \vartheta = 2.8$ mrad

3.4.2. c Dependence on two -photon detuning δ

For lower pump power and choosing angle $\vartheta = 2.8$ mrad, gains of beams are calculated for different two photon detuning δ see fig.11. For lower pump power there is no preferred angle, gains have maximums indicating that lower pump moves peal position to smaller TPD also the

maximum gain depending on cell length. The gain for longer cell is higher and the peak is wider than the shorter cell.

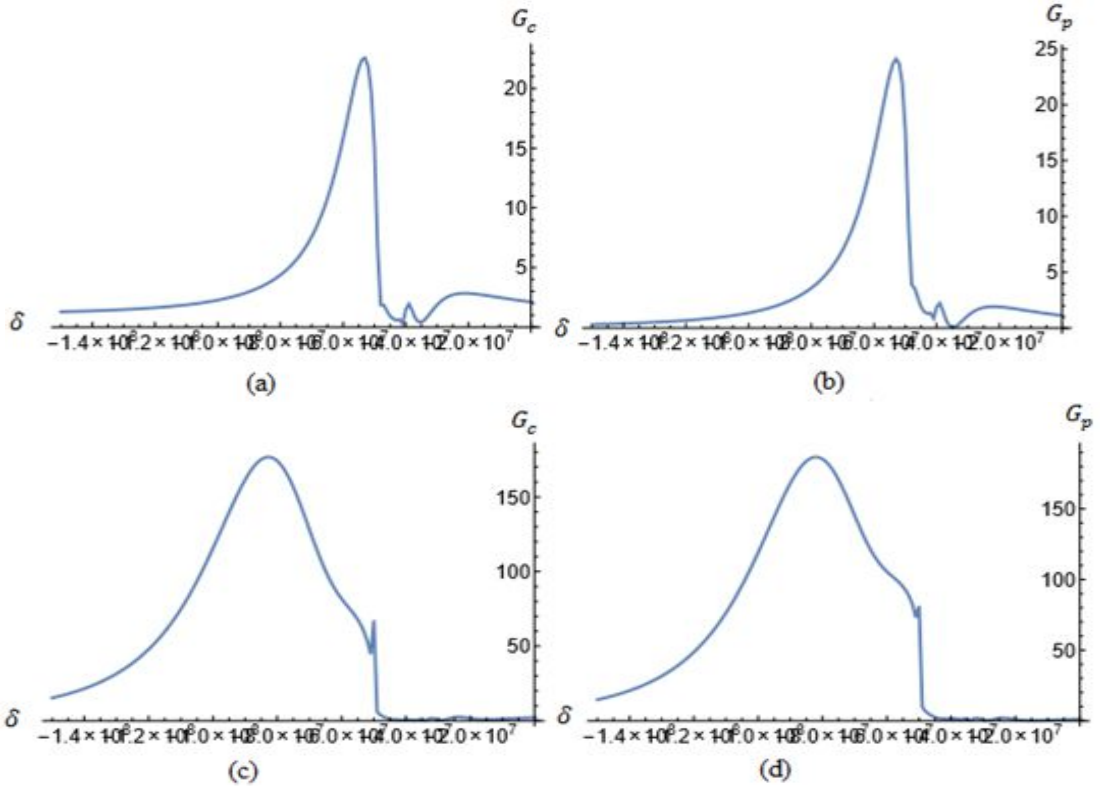

FIG.11. Calculated effects of pump power on conjugate and probe beams as a function of two photon detuning δ, $\Omega = 1.94$ GHz, $\mathrm{Nc} = 1 * 10^{18}\mathrm{cm}^{-3}$.

For 1cm cell (a, b). $\delta = -0.60 * 10^{8}$, $\Delta = 1\mathrm{GHz}, \vartheta = 2.8$ mrad.

For 4cm cell (c, d). $\delta = -0.90 * 10^{8}$, $\Delta = 1\mathrm{GHz}, \vartheta = 2.8$ mrad.

3.4.3 Additional results for Thin cell, Medium pump Intensity

We show in this part the results of gains of twin beams of we got with these common parameters:

propagation distance $\mathrm{zmax} = 1\mathrm{cm}$, electric field amplitude of the pump $\mathrm{E}_{\mathrm{d}}^{(+)} = 6000\frac{\mathrm{N}}{\mathrm{C}}$, that corresponds to Rabi frequency Omega

$\Omega_d = 1.94$ GHz and electric field amplitude of the probe $E_P^{(+)} = 71.9 \frac{N}{C}$, that corresponds to Rabi frequency Omega $\Omega_P = 22.6$ MHz, electric field amplitude of the conjugate is $E_c^{(+)} = 1$, that corresponds to Rabi frequency Omega $\Omega_c = 330$ KHz, gamma $\gamma = 10^1$ MHz and depasing rate $\gamma_{deph} = 3 * 10^4$MHz, atom density is $Nc = 1 * 10^{18} cm^{-3}$, one-photon detuning is $\Delta = 2 * pi * 0.8 * 10^9$ GHz, $\Delta = 2 * pi * 1.2 * 10^9$GHz ,anglels between pump and probe and pump and conjugate $\vartheta = 2.8$ mrad, two photon detuning for thin cell is $\delta = -1.2 * 10^8$ MHz, $\delta = -0.30 * 10^8$ MHz.

3.4.3.a Dependence on Two Photon Detuning (TPD) For Lower and Higher One Photon Detuning (OPD)

We have calculated gains vs TPD, for different OPD, and gains vs OPD for several TPD for pump power and 1cm cell. Increasing OPD, shifts values of TPD corresponding to the gain maximums to smaller TPD, while increasing TPD moves gain maximums to smaller OPD see figures 12, 13.(a, b, c, d).

Dependence of gains of twin beams in terms of two photon detuning for different one photon detunings values for pump power and 1cm cell are presented in Fig. 12(a, b, c, d). The maximum of gains are at maximum two photon detuning δm depend on one-photon detuning and for all other

parameters fixed, it is more negative if one photon detuning Δ is smaller see figures. This is a clear evidence of the differential Stark shift. Hyperfine energy levels have different Stark shifts from off-resonant pump. The maximum of gain is at this differential shift. It is dependent on OPD which is the train known from the theoretical analysis of a two level atomic system.

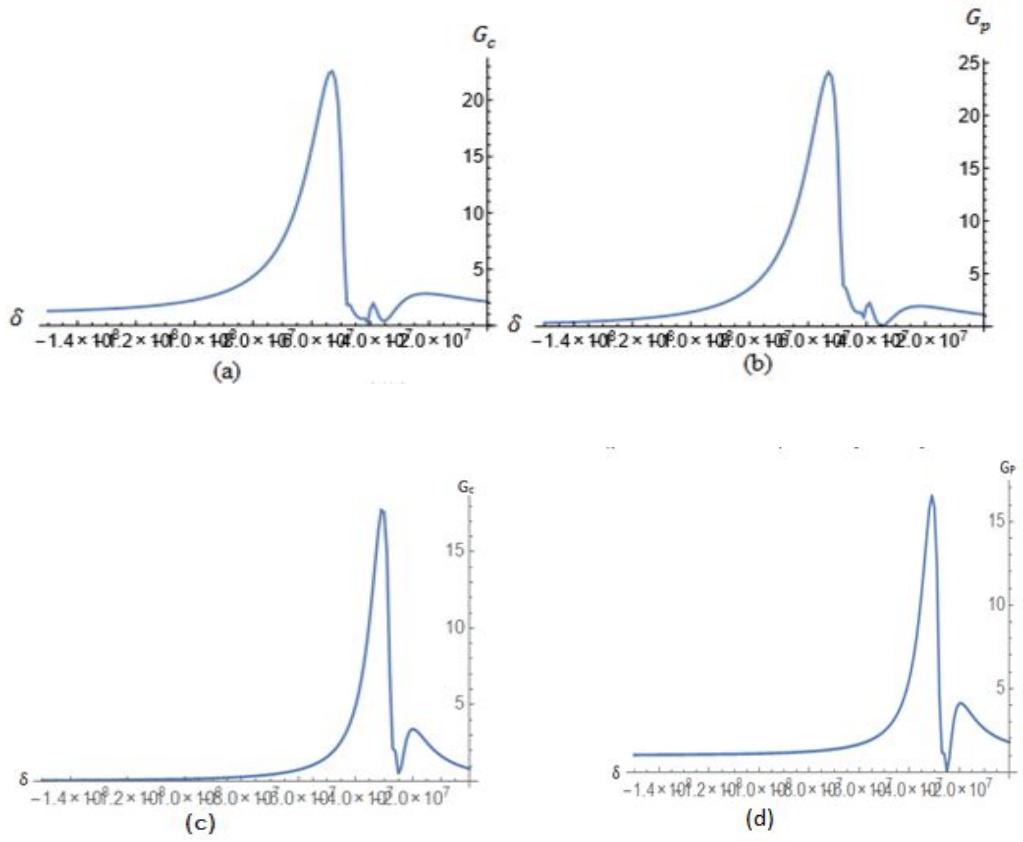

Figure 12(a, b). Calculated gain of the conjugate and probe beams dependence on TPD for lower one photon detuning.

Figure 12(c, d). Calculated gain of the conjugate and probe beams dependence on TPD for higher OPD, $\delta = -0.60 * 10^8, \vartheta = 2.8$ mrad, $N_c = 1 * 10^{18}\text{cm}^{-3}, \Delta = 2 * \text{pi} * 0.8 * 10^9\text{GHz}, \Delta = 2 * \text{pi} * 1.2 * 10^9\text{GHz}$.

3.4.3.b Dependence on One Photon Detuning (OPD) for Lower and Higher Two Photon Detuning (TPD)

Calculated results of gains as a function of one-photon resonance Δ for lower and higher two photon detunings are given in Fig.13(a, b, c, d). One-photon detuning for maximum gains, Δm, are close to 1GHz but this value moves around depending on the value of δ, slight move of Δm towards lower values when δ is larger. Not presented in the Figure 13. but the numerical simulations shows weekly or no dependence of the position of the maximum on the angle between the pump and probe.

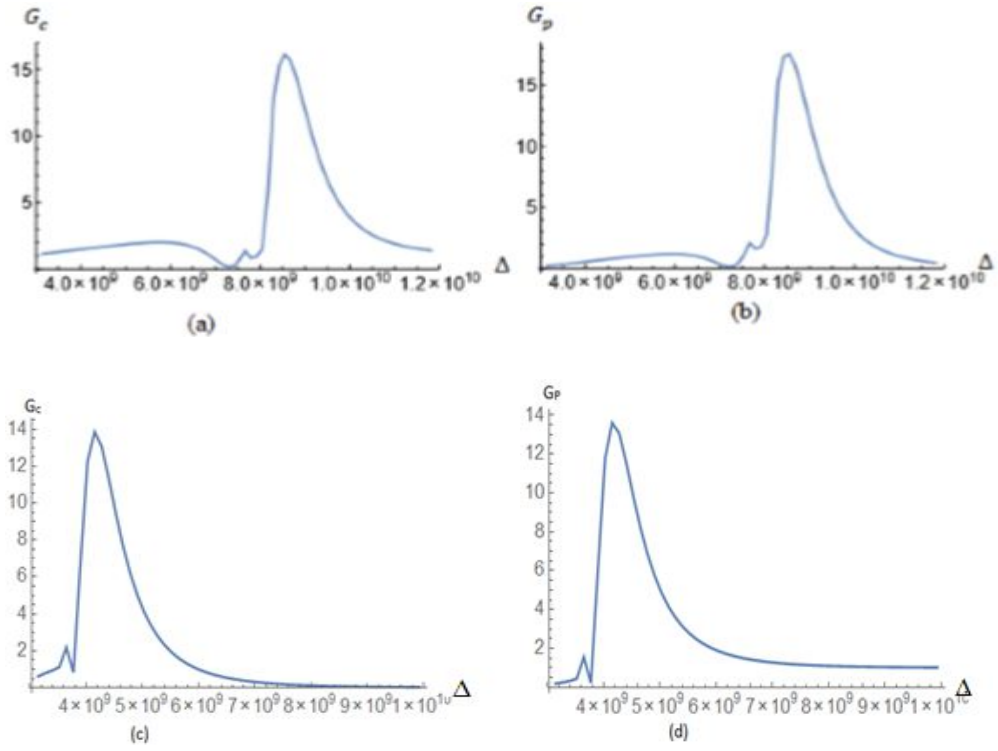

Figure 13(a, b). The probe and conjugate and beams' calculated gain depending on OPD for lower two photon detuning. Figure 13(c, d). The probe and conjugate beams' calculated gain dependence on OPD for higher TPD, $\delta = -0.30 * 10^8, \delta = -1.2 * 10^8, \Delta = 2 * pi * 0.8 * 10^9 GHz$.

3.4.4 Dependence on probe power

The based on the probe power gain is not so pronounced. It varies slowly with higher input probe power leads to lower and lower gains. This may be attributed to the saturation in FWM. Gains are defined as quotient of intensities of the output beam and input probe. If some side effect limits the output intensity then this quotient will go down for higher input probe power.

Chapter 4

4. Results

This chapter contains the presentation the numerical simulations results in the two cases; with Doppler averaging and [32] without Doppler averaging of density matrix components and compare it to measurements. By using the D1 line transition of potassium vapor and we will use the double lambda Λ atomic scheme under conditions of potassium vapor's four wave mixing under condition full width at a half maximum determined by value equal 80ns. So therefore we have identified set of parameters such as detuning of one-photon pump also detuning of two-photon probe-pump Raman, and vapor density, laser powers and Rabi frequencies, where pump intensity is set to be constant over time while probe forms a pulse. And the comparison will be presented comparison between results without Doppler averaging and the results with Doppler normalizing of density matrix components.

In order to [31] consider Doppler normalizing of density matrix components we divide the atom velocity distribution into different number of M [32] groups, each with different z-projection of velocity υ_z [24]. Owing to the Doppler effect, such groups vary in efficient detuning. Modified propagation equations read:

$$\left(\frac{\partial}{\partial \mathrm{z}}+\frac{1}{c}\frac{\partial}{\partial t}\right)E_d^{(+)}=\sum_{m=1}^{M}\frac{kN_{c,k}}{2\varepsilon_0}\,d\left(\tilde{\varrho}_{42,m}+\tilde{\varrho}_{31,m}\right),$$

$$\left(\frac{\partial}{\partial z}+\frac{1}{c}\frac{\partial}{\partial t}\right)E_d^{(+)}=\sum_{m=1}^{M}\frac{kN_{c,k}}{2\varepsilon_0}\,d\tilde{\varrho}_{32,m},$$

$$\left(\frac{\partial}{\partial z}+\frac{1}{c}\frac{\partial}{\partial t}\right)E_d^{(+)}=\sum_{m=1}^{M}\frac{kN_{c,k}}{2\varepsilon_0}\,d\tilde{\varrho}_{41,m}.$$

The quantity $N_{c,k}$ is the atom density of the K -th group; c is speed of light, we choose $\upsilon_{z,m}$and $N_{c,m}$ to mimic Maxwell distribution

$$f(\upsilon_z)=\sqrt{\frac{m}{2\pi KT}}\,e^{-\frac{m\upsilon_z^2}{2KT}}.$$

Moreover furthermore we will use with the Doppler averaging M groups equal three. We will firstly solve motionless system whereby we set the t=0 in the initial condition for Maxwell Bloch equation of probe field where is determined by equation

$$E_d^{(+)}=E_{P^0}^{(+)}(f_{DC}+f_{pluse}e^{-\frac{4In2(t-t_{max})^2}{FWHM^2}})$$

In which represent time when the pulse attains peak value, FWHM is the total width at semi maximum, t_{max} and f_{DC} and f_{pluse}adds to one and represent DC and pulse components. Dependencies of z are obtained for all unidentified variables, and it will be see results obtained for the conjugate and probe beam of dependence on time and z direction

4.1 Figure and discussion

We analyze the results obtained with Maxwell Block equations for some range of parameters where Pump intensity is set to be constant over time and whilst probe forms a pulse for a certain set of parameters these one

photon detunings are in a the GHz range, whilst the two photon detunings are in the negative values of MHz range.

We begin by present the first results that consists of the output pulses that are still bell shaped, it will be like same (Gaussians), from these shapes we can get results like fractional delays and broadening. It will be necessary to mention the set of parameters used to in the model describes of the interaction between isotopes of potassium mass number 39 in the vapor and electromagnetic field.

Where these parameters are determined by values following:

The propagation distance $\mathrm{zmax} = 4\mathrm{cm}$, one-photon detuning is $\Delta = 0.7\mathrm{GHz}$, two- photon detuning is $\delta = -2\pi 8\mathrm{MHz}$, gamma is $\gamma = 0.5 \,.\, 10^{7}$ MHz, and depasing rate $\gamma_{\mathrm{deph}} = 1.5 \,.\, 10^{7}$, atom density is $\mathrm{Nc} = 3 \,.\, 10^{12}\mathrm{cm}^{-3}$, the temperature $\mathrm{T} = 120^{0}\mathrm{C}$, anglels between pump and probe and pump and conjugate equal to $\vartheta = 3$ mrad, electric field amplitude of the pump $\mathrm{E}_{\mathrm{d}}^{(+)} = 6998.62\,\frac{\mathrm{N}}{\mathrm{C}}$ Rabi frequency (Omega) for pump is determined value $\Omega_{\mathrm{d}} = 3.08$ GHz, and electric field amplitude of the probe $\mathrm{E}_{\mathrm{P}}^{(+)} = 57.28\ \frac{\mathrm{N}}{\mathrm{C}}$ also rabi frequency (Omega) for probe is determined value $\Omega_{\mathrm{P}} = 18.9$ MHz, where total width at probe beam's semi maximum (FWHM) equal to 80ns, electric field amplitude of the conjugate is $\mathrm{E}_{\mathrm{c}}^{(+)} = 1$, that corresponds to Rabi frequency Omega $\Omega_{\mathrm{c}} = 330$ KHz.

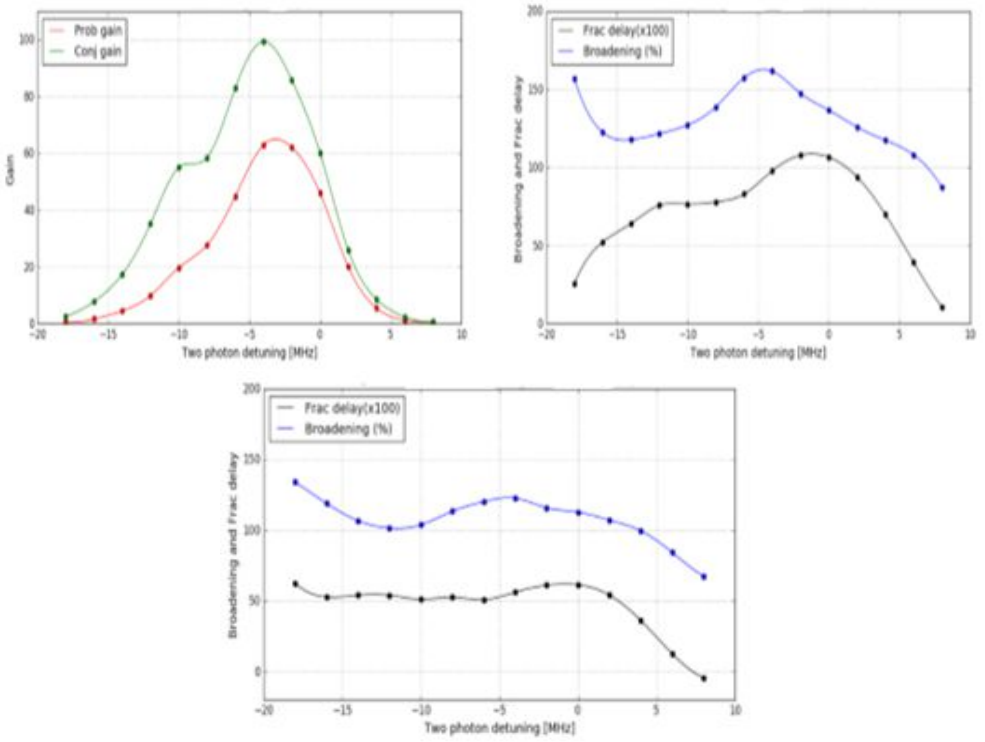

Fig. 14. Measurement Probe and conjugate beams, (1) gains depend on two photon detuning also (2) fractional broadenings depend on two photon detuning and (3) fractional delays depend on two photon detuning, for $\Delta = 0.7GHz, T = 120C^0$, pump power P_d = 220mW, probe power P_p = 20 μW.

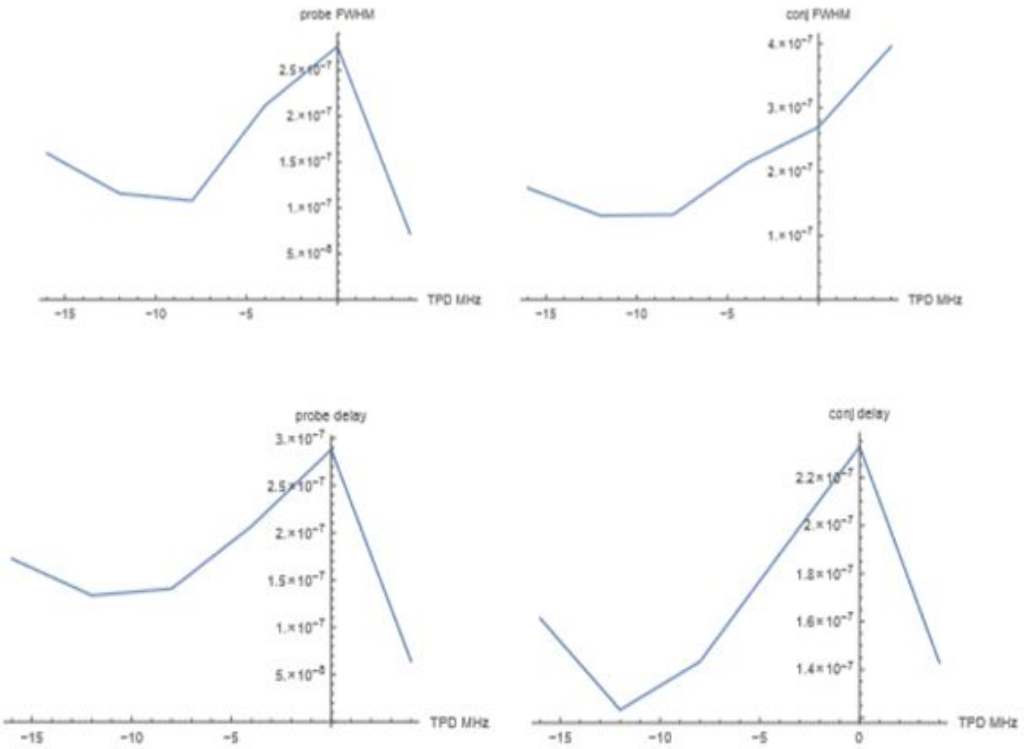

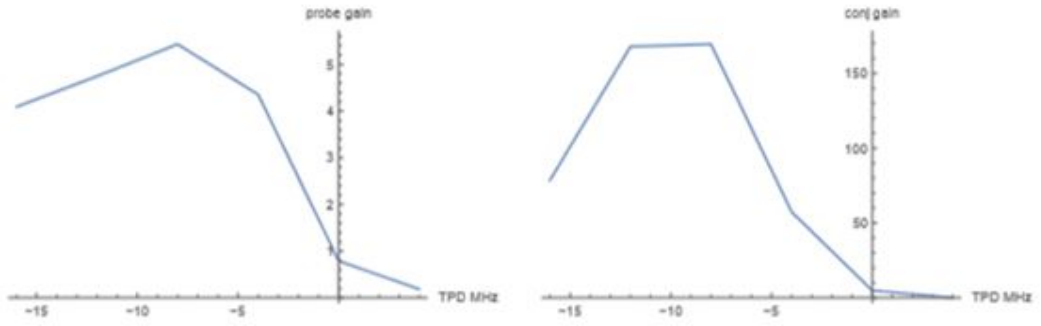

Fig. 15. Calculated probe and conjugate beams incoming from with Doppler averaging effect depended on two photon detuning (1) for gains (2) also for fractional delays, (3) and for fractional broadenings, for $\Delta = 0.7GHz, T = 120C^0$, pump power P_d = 220mW, probe power P_p = 20 μW.

In the model we choose parameters to relate to the experimental values such as detunings between probe and pump and gas density. It also uses variables with unknown values in the measurements, including relaxation coefficients. Better compliance with measurements was obtained in case the amplitudes of electric field in the design are a slightly below the one implied by the measurement. When compare between measurement and the model with Doppler averaging we note the both gains peak maximized at some negative value of two photon detuning in the MHz range. Delays and broadening are also dependent on δ. Not only the measurements, but also the model exhibit further deviations from Gaussian systems when the gains are lower or when atomic densities are higher. Figures 14 and 15. Show typical behavior of figures of merit for probe and conjugate pulses both experimentally and theoretically. Experimental data [24] shows tendencies in FWHMs, gains and delays

for the conjugate and probe. Numerical simulations agrees properly with measurements.

4.1.1 Probe pulses Propagation through potassium vapor cell

We show example of pulse destruction and revival through potassium vapor cell of 4cm parameters for the simulations:

While one-photon detuning is $\Delta = 0.7$GHz, two- photon is determined by value $\delta = -2$MHz, gamma is $\gamma = 0.5 \cdot 10^7$ MHz, and depasing rate $\gamma_{deph} = 1.5 \cdot 10^7$, atom density is $Nc = 3 \cdot 10^{12}\text{cm}^{-3}$, the temperature $T = 120^0 C$, anglels between pump and probe and pump and conjugate equal to $\vartheta = 3$ mrad, electric field amplitude of the pump $E_d^{(+)} = 6998.62 \frac{N}{C}$ Rabi frequency (Omega) for pump is determined value $\Omega_d = 3.08$ GHz, and electric field amplitude of the probe $E_P^{(+)} = 57.28 \frac{N}{C}$ also rabi frequency (Omega)for probe is determined value $\Omega_P = 18.9$ MHz, where total width at probe beam's semi maximum (FWHM) equal to $80ns$, electric field amplitude of the conjugate is $E_c^{(+)} = 1$, that corresponds to Rabi frequency Omega $\Omega_c = 330$KHz.

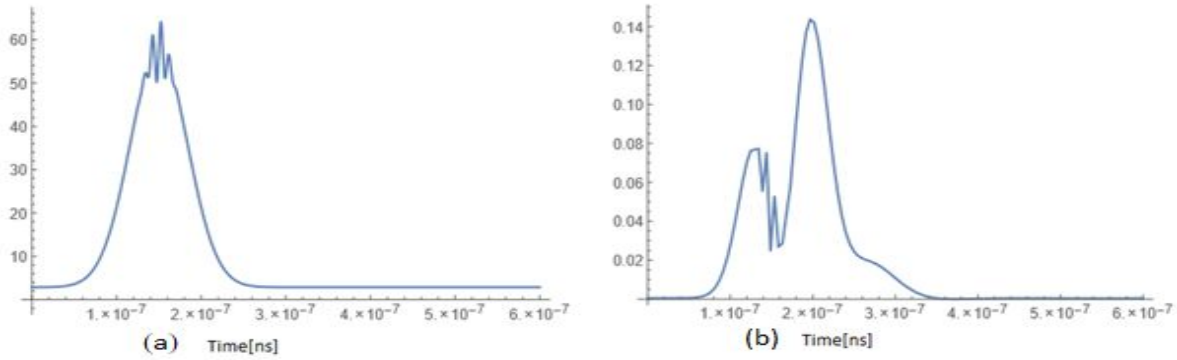

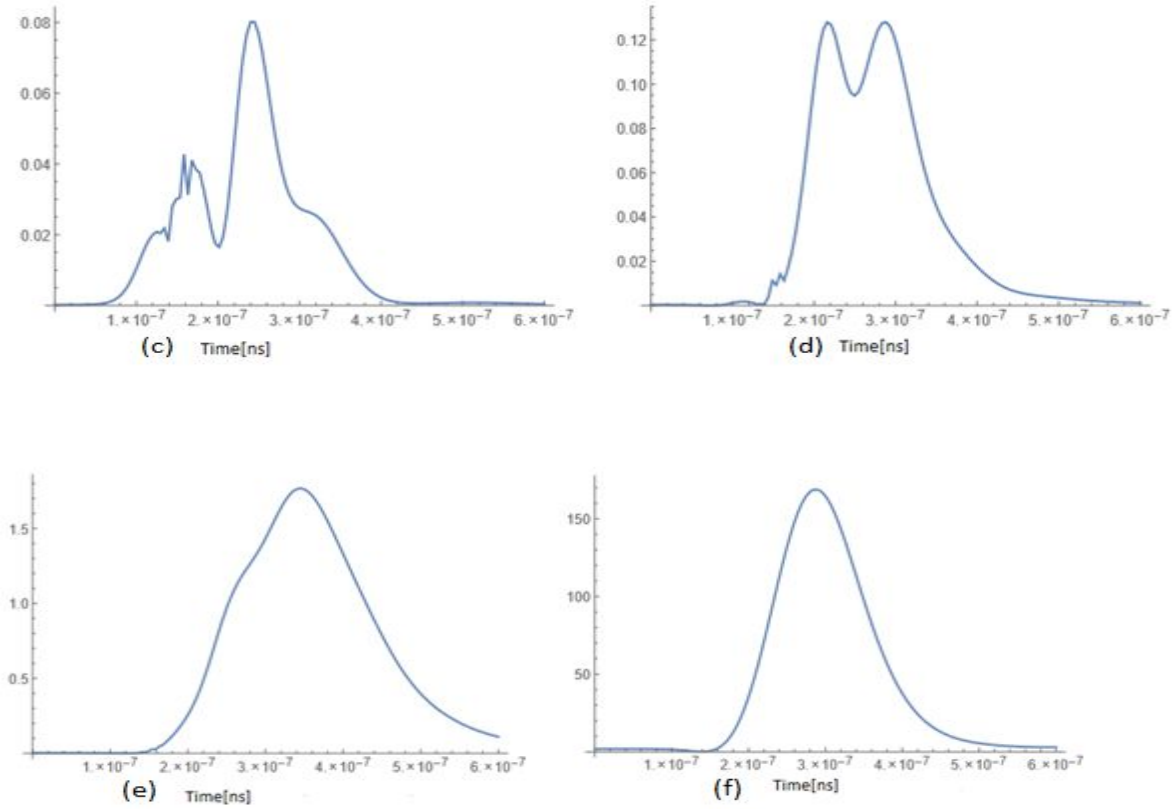

Fig.16. Example of 80ns probe pulse destruction and revival through potassium vapor cell of 4cm, Pulse waveforms at (1) [41] z = 0*zmax, (2) z= 0.08*zmax, (3) z= 0.16*zmax, (4) z=0.24*zmax, (5) z=0.52*zmax, (6) z= zmax percentage of the total cell length. Parameters for simulations: $\Delta = 0.7\text{GHz}, \delta = -2\text{MHz}$,gamma is $\gamma = 0.5.10^7\text{MHz}$, and depasing rate $\gamma_{deph} = 1.5.10^7$, density of corn is $Nc = 3.10^{12} cm^{-3}$, the temperature $T = 120^0 C$.

The top part of probe pulse was added wavelet small at the probe pulse input after running numerical simulation to see the dynamics of the probe pulses, we note the shape of probe take bell form at the input and also at the output, also they are not directly connected by a time evolution and behind the initial pulses begin additional secondary pulses to continue to appear with sufficient gains at the end of the propagation distance, the mission these additional secondary pulses only are responsible for slow

light and expanding pulses. By return to the [32] marker location on the top profile Gaussian pulse, it was noted that primary pulse disappears at the exit from cell.

4.1.2 Determination both primary and secondary pulse at the end of the propagation distance zmax= 4cm for some parameters

Results are for the following parameters:

1-photon detuning is $\Delta = 1.3$ GHz and 2- photon detuning can be determined by four values four values $\delta = (2\pi 4\text{MHz},\ 0\text{MHz},\ -2\pi 4\text{MHz}, -2\pi 8\text{MHz})$, gamma is $\gamma = 0.5 \cdot 10^{7}$MHz ,and depasing rate $\gamma_{\text{deph}} = 1.5 \cdot 10^{7}$, atom density is $\text{Nc} = 3 \cdot 10^{18}\text{cm}^{-3}$, the temperature $T = 120^{0}C$, anglels between pump and probe and pump and conjugate equal to $\vartheta = 3$mrad, electric field amplitude of the pump $\text{E}_{\text{d}}^{(+)} = 6998.62\,\frac{\text{N}}{\text{C}}$ Rabi frequency (Omega) for pump is determined value $\Omega_{\text{d}} = 1.377$GHz, and electric field amplitude of the probe $\text{E}_{\text{P}}^{(+)} = 57.28\ \frac{\text{N}}{\text{C}}$ also rabi frequency (Omega)for probe is determined value $\Omega_{\text{P}} = 1.19$ MHz, where total width at probe beam's semi maximum (FWHM) equal to $80ns$, electric field amplitude of the conjugate is $\text{E}_{\text{c}}^{(+)} = 1$, that corresponds to Rabi frequency Omega $\Omega_{\text{c}} = 330$KHz.

First, we present the results obtained theoretically with and without

Doppler averaging and compare them by measurement.

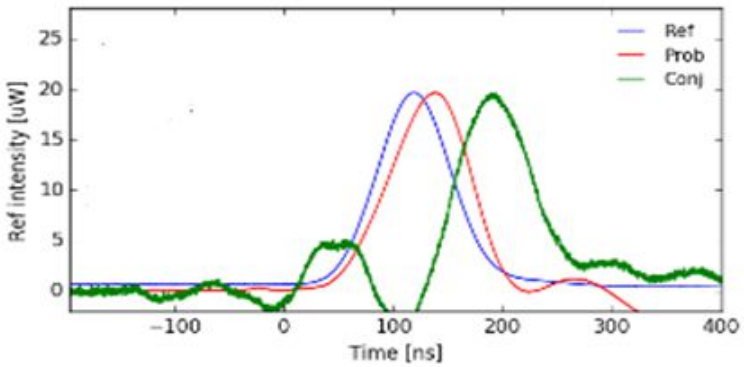

Figure 17. Investigational analysis of slow light – conjugate (green), probe (red), and reference 80 ns inbound probe beam (blue) two photon detuning waveforms δ = 2π4MHz, one photon detuning Δ = 1.3 GHz, temperature $T = 120^0 C$, pump power P_d = 220mW, probe power P_p = 20 μW, $\Omega_d = 1.377$ GHz , $\Omega_P = 1.19$ MHz

There are is qualitatively different outputs for all lines, probe (red), conjugate (green) and reference 80 ns incoming probe beam (blue) there is a numerical comparison where theory gives similar result and switching to the nearby set of parameters yields to more Gaussian-like output see figure 17 we note there is a delay (slow light) for both probe and conjugate lines.

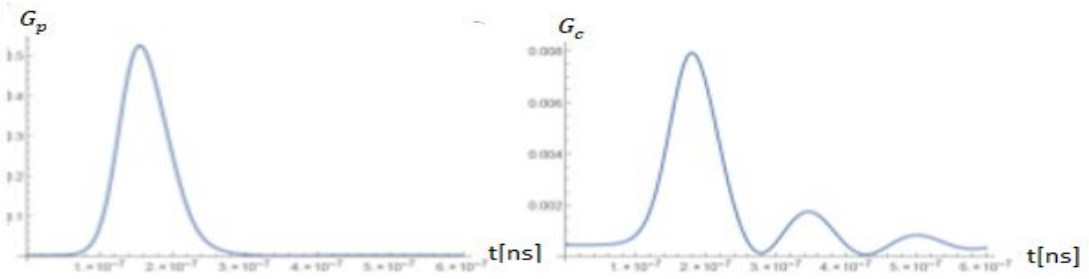

FIG. 17a. Conjugate and probe waveforms numerical simulations without Doppler averaging. 80 ns probe incoming pulse results, Δ = 1.3 GHz, and δ = 2π4MHz. Additional factors for simulations:$\Omega_d = 1.377 GHz$, $\Omega_P = 1.19\ MHz$,$Nc = 3.10^{18} cm^{-3}$,$\gamma = 0.5.10^7 MHz$,$\gamma_{deph} = 1.5.10^7$.

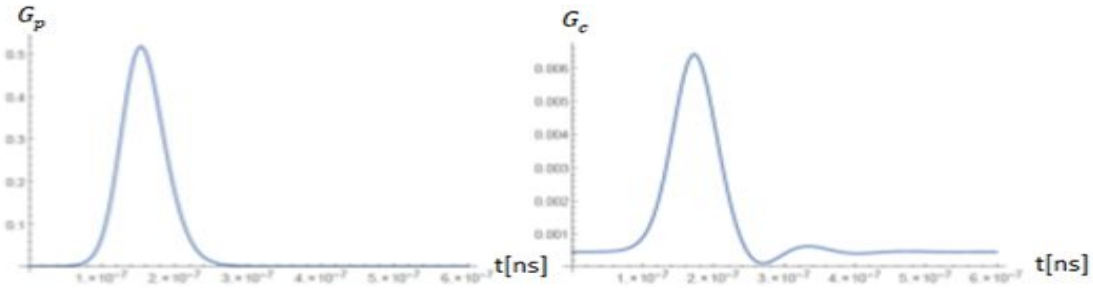

FIG. 17b. Conjugate and probe waveforms numerical simulations with Doppler averaging. Results are parameters for 80 ns, Δ = 1.3 GHz, and δ = 2π4MHz. $\Omega_d = 1.377GHz,\ \Omega_P = 1.19MHz$,$Nc = 3.10^{18}cm^{-3}$,$\gamma = 0.5.10^{7}MHz$,$\gamma_{deph} = 1.5.10^{7}$.

Numerical simulations results example, with or without Doppler normalizing, and measurement with the FWHM of the probe beam equal to 80nm and for four various values of two photon detuning where $\delta = 2\pi 4MHz, 2\pi 0MHz, -2\pi 4MHz, -2\pi 8MHz$, and one photon detuning is determined by value 1.3GHz for all figures are presented here.

We start with figures17, 17a, 17b for TPD = 2π 4MHz we note the results for numerical simulations of both probe and conjugate waveforms with and with no Doppler averaging theory and measurement gives almost no deformation pluses for probe and diminishing secondary pulses for conjugate.

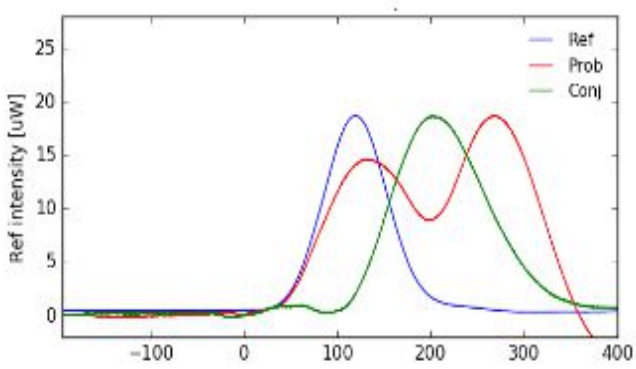

Figure 18. Observations through experimentation of conjugate (green) and slow light – probe (red), reference 80 ns inbound probe beam (blue) two photon detuning waveforms δ = 0 MHz, one photon detuning Δ = 1.3 GHz, temperature T = 120C0, pump power Pd = 220 mW, probe power Pp = 20 μW,$\Omega_d = 1.377GHz$,$\Omega_P = 1.19MHz$.

Also there are is qualitatively different outputs for all lines, probe (red), conjugate (green) and reference 80 ns incoming probe beam (blue) moreover, there is a numerical comparison where theory gives similar result and switching to the nearby set of parameters yields to more Gaussian-like output see figure 18, we note conjugate experienced both primary and secondary pulse. Secondary probe pulse is slower than conjugate.

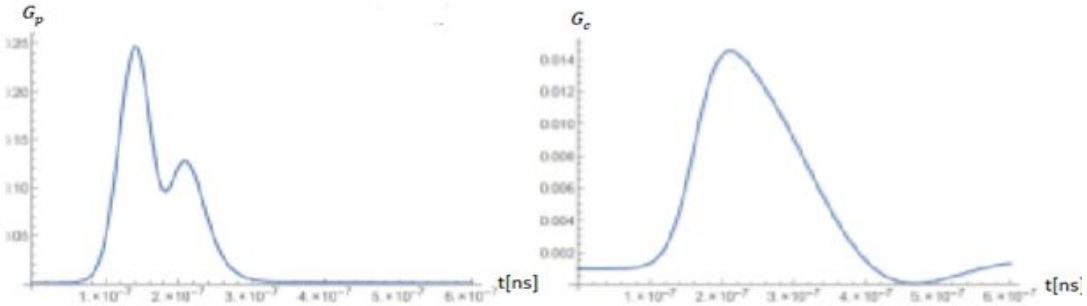

18a. Probe and conjugate waveforms' numerical simulations no Doppler averaging of parameters for simulations are: FWHM= 80 ns, Δ = 1.3 GHz and δ = 0MHz. Other parameters

for simulations: $\Omega_d = 1.377GHz$,

$\Omega_P = 1.19MHz, Nc = 3.10^{18}cm^{-3}, \gamma = 0.5.10^7 MHz, \gamma_{deph} = 1.5.10^7$

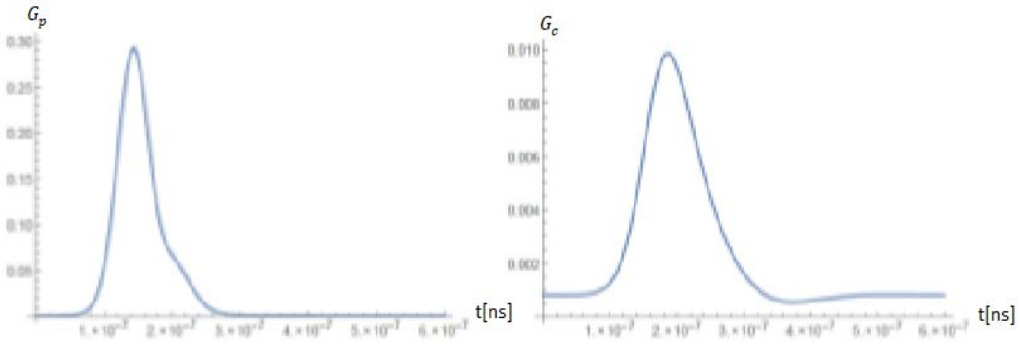

FIG.18b. probe and conjugate waveforms' numerical simulations with Doppler averaging effect the results are for: 80 ns, Δ = 1.3 GHz and δ = 0MHz, $\Omega_d = 1.377GHz$, $\Omega_P = 1.19MHz, Nc = 3.10^{18}cm^{-3}, \gamma = 0.5.10^7 MHz, \gamma_{deph} = 1.5.10^7$

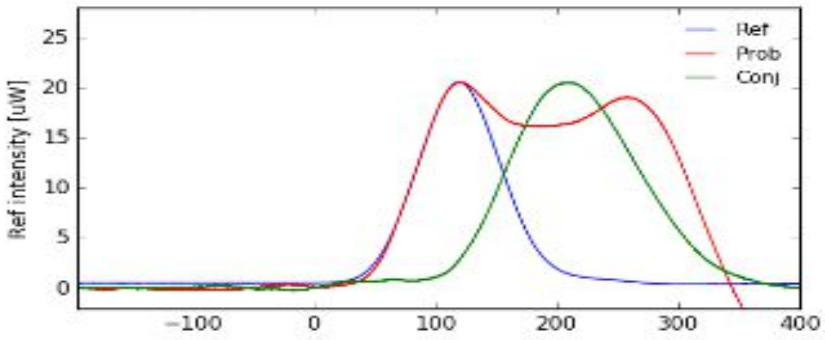

Figure 19. Experiment of slow light – conjugate (green), probe (red), and reference 80ns inbound probe beam (blue) waveforms for two photon detuning δ = −2π4MHz, one photon detuning Δ = 1.3GHz, temperature T = $120C^0$, pump power P_d = 220 mW, probe power P_p = 20 μW, $\Omega_d = 1.377$ GHz , $\Omega_P = 1.19$ MHz.

In figure 19, there is qualitatively very [42] different conjugate and probe's waveforms at the cell exit. Also there is a numerical comparison where theory gives similar result and switching to the nearby set of parameters yields to more Gaussian-like output, where we note conjugate

experienced both primary and secondary pulse. Secondary probe pulse is slower than conjugate.

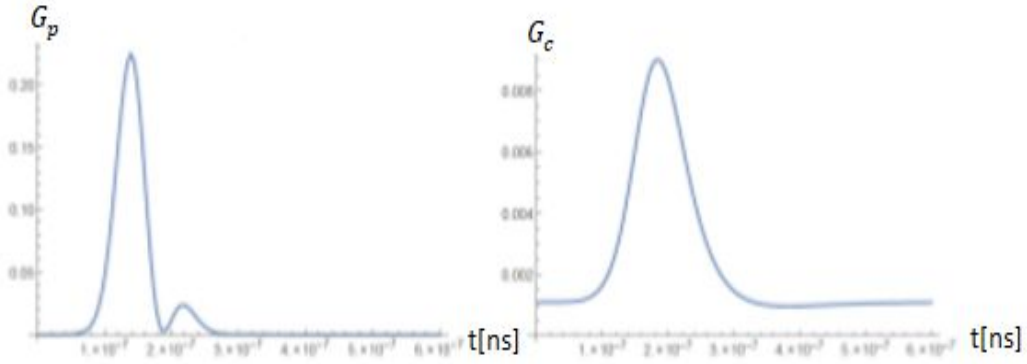

FIG. 19a. Results of numerical simulation of probe and conjugate waveforms with Doppler averaging for parameters are: FWHM=80 ns, Δ = 1.3GHz, and δ = - 2π4MHz. $\Omega_d = 1.377GHz$, $\Omega_P = 1.19MHz$, $Nc = 3.10^{18}cm^{-3}$, $\gamma = 0.5.10^7 MHz$, $\gamma_{deph} = 1.5.10^7$

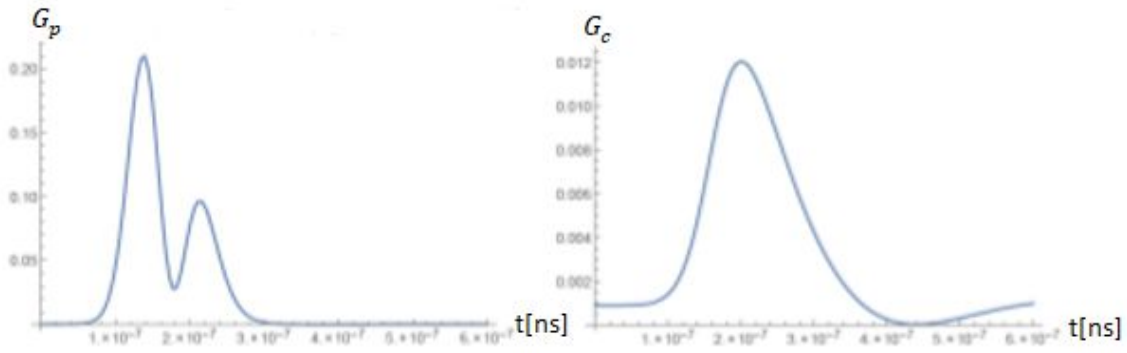

FIG. 19b. Probe and conjugate waveforms' Numerical simulations without Doppler averaging for these parameters: FWHM= 80 ns, Δ = 1.3 GHz, and δ = -2π4MHz, $\Omega_d = 1.377GHz, \Omega_P = 1.19MHz$, $Nc = 3.10^{18}cm^{-3}$,$\gamma = 0.5.10^7 MHz$, $\gamma_{deph} = 1.5.10^7$.

In the case lower value for two photon detuning see figure 15, 15a, 15b and figure16, 16a, 16b where $\delta = 0MHz \wedge -2\pi 4MHz$, we note the resultes for probe and conjugate waveforms' numerical simulations with and with no Doppler averaging and measurement there are primary waves and secondary waves present with probe beam while conjugate beam

consists of one peak at the end of the propagation distance.

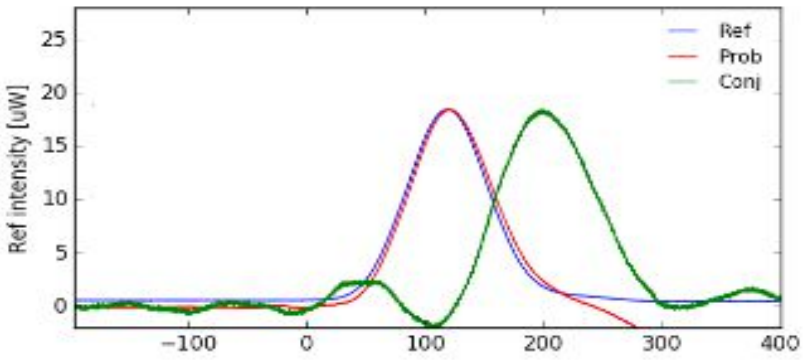

Figure 20. Experimental illustration of slow light – conjugate (green), probe (red), and reference 80 ns inbound probe beam (blue) waveforms for two photon detuning δ = −2π8MHz, one photon detuning Δ = 1.3GHz, temperature T = 120 C^0, pump power Pd = 220mW, probe power Pp = 20μW,$\Omega_d = 1.377GHz$,$\Omega_P = 1.19MHz$.

Looking at the figure 20, we there is note qualitatively different waveforms for the probe (red) and the conjugate (green) at the cell exit. Also there is a numerical comparison where theory gives similar result and switching to the nearby set of parameters yields [32] to more Gaussian-like output, where we note the probe is almost unchanged while the conjugate is slow. Lower gains more frequently lead to irregular results. Not only measurements, but also the model exhibit further deviations from Gaussian systems when the gains are lower or when atomic densities are higher.

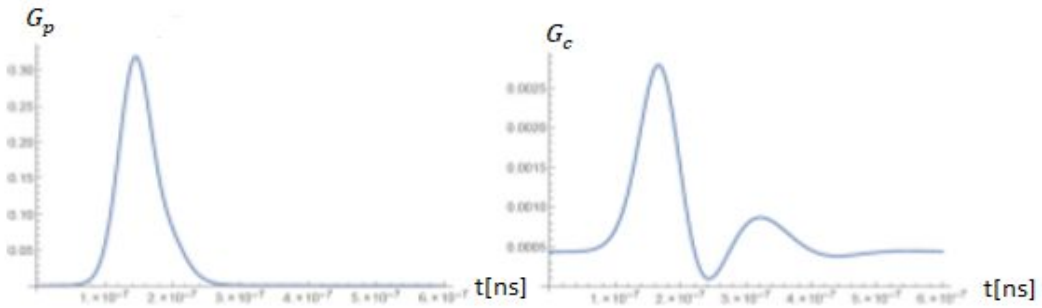

FIG. 20a. Results for probe and conjugate waveforms with Doppler averaging, in the case numerical simulations by using these parameters: FWHM=80 ns, Δ = 1.3 GHz, and δ = -2π8MHz, $\Omega_d = 1.377GHz$, $\Omega_P = 1.19MHz$,$Nc = 3.10^{18}cm^{-3}$, $\gamma = 0.5.10^7 MHz$, $\gamma_{deph} = 1.5.10^7$

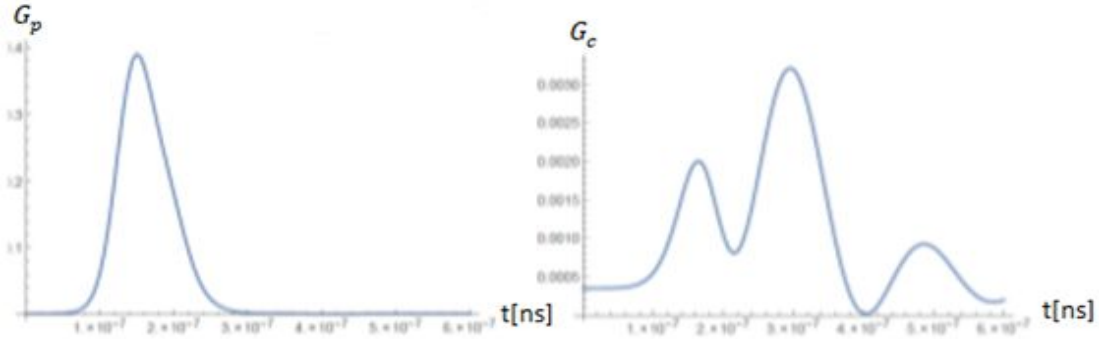

FIG. 20b. Results of numerical simulations incoming from waveforms for probe and conjugate in state without Doppler averaging by using these parameters: FWHM=80 ns, Δ = 1.3 GHz, and δ = -2π8MHz, $\Omega_d = 1.377GHz, \Omega_P = 1.19MHz$,$Nc = 3.10^{18}cm^{-3}$,$\gamma = 0.5.10^7 MHz$,$\gamma_{deph} = 1.5.10^7$,$\gamma_{deph} = 1.5.10^7$

Finally, figure 20, 20a, 20b for two photon detuning equal δ=-2π8MHz where we see in the both theory and measurement no deformation wave for probe at the end of propagation distance and the conjugation beam has its secondary pulse diminishing it similar result for figure 17, 17a, 17b.

CONCLUSION

This thesis describes the phenomenon of four waves mixing in atomic potassium vapor mass number 39 and also we present results of numerical calculations for propagation of effects twin beams during of the hot [32] potassium (K) vapor and make comparison between measured and calculated gains for a broad range of variables necessary for FWM efficiency. This is inclusive of the atomic density, angle between the probe and the pump, two photons detuning, and detuning of the pump from the D1 transition, with respect to hyperfine structure of the ground. Finding relations between different parameters and gains because gain is directly related to the amount of squeezing and of entangled photons. Numerically, we use full system of Maxwell Bloch equations used to calculate density matrix terms of every population and coherence to determine atomic polarization induced by the propagation expressions for amplitudes of three modes of electric fields conjugate, pump and probe.

It known to be four wave mixing in a potassium vapor characterized by distorting the pulse beams. Through this feature we analyze the results obtained with Maxwell Bloch mode for some range of parameter and we will demonstrate it with propagation of full width at a half maximum of the conjugate and probe beams equal to 80nm in the K vapor under FWM

generated by the double Λ scheme under for a certain some range of parameters gains such as 1-photon detuning and 2-photon detuning, also gas densities. The pluses' shape can be bell shaped for some detuning like (Gaussian) or deformed or very different shapes at the end of the propagation distance this is in agreement with measurements and from such waveforms we obtain the shapes for pulse's gains, delays and broadening.

References

[1] B. Zlatkovic, A. J. Krmpot, N. Sibalic, M. Radonjic, B. M. Jelenkovic, Laser Physics. Letters 13, 015205 (5pp) (2016).

[2] M. T. Turnbull, P. G. Petrov, C. S. Embrey, A. M. Marino, and V. Boyer, Phys. Rev. A 88, 033845 (2013).

[3] http://www.tobiastiecke.nl/archive/PotassiumProperties.pdf.

[4] A. Eilam, A. D. Wilson-Gordon, and H. Friedmann, Optics Letters 33(14) (2008).

[5] Ken-ichi Harada, Tatsuya Kanbashi, Masaharu Mitsunaga, Koji Motomura, Phys. Rev. A 73, 013807 (2006).

[6] Q. Glorieux, R. Dubessy, S. Guibal, L. Guidoni, J. -P. Likforman, and T. Coudreau, E. Arimondo, Phys. Rev. A 82, 033819 (2010).

[7]http://community.dur.ac.uk/thomas.billam/PreviousNotes_MPAJones.pdf.

[8] https://ocw.mit.edu/courses/electrical-engineering-and-computer-science/6- 974-fundamentals-of-photonics-quantum-electronics-spring-2006/lecture- notes/chapter6.pdf .

[9] F. E. Becerra, R. T. Willis, S. L. Rolston, and L. A. Orozco, Phys. Rev. A 78.013834 (2008).

[10] C. Goren, A. D. Wilson-Gordon, M. Rosenbluh, and H.Friedmann, Phys. Rev. A 69, 053818 (2004).

[11] Peatross, Justin, Michael Ware. Physics of Light and Optics. Brigham Young University: Peatross and Ware,2004-2008.

[12] A. V. Taichenachev, A. M. Tumaikin, and V. I. Yudin, Phys. Rev. A 61, 011802 (1999).

[13] R. T. Willis, F. E. Becerra, L. A. Orozco, and S. L. Rolston, Phys. Rev. A79, 033814 (2009).

[14] W. Boyd, Robert. Nonlinear Optics Second Edition. The institute of Optics University of Rochester: Elsevier Science(USA),2003.

[15] Marlan O. Scully, M. Suhail Zubairy. Quantum Optics. Cambridge University Press: United Kingdom,1997.

[16] Steck, Daniel Adam. Quantum and Atom Optics. Oregon Center for Optics and Department of Physics, University of Oregon: By Daniel Adam Steck,2007.

[17] Michael Fleichhauer, Atac Imamoglu, and Jonatgan P. Marangos, RevModPhys. 77.633 (2005).

[18] Louden,Rodney. The Quantum Theory of Light Third Edition. Oxford University of press: United States,2000.

[19] B. E. King, Phys. Atom- Ph. 0804.4528 (2008).

[20] Ken-ichi Takahashi, Nobuhito Hayashi, Hiroaki Kido, Shota

Sugimura, Naoya Hombo, and Masaharu Mitsunaga, Phys.Rev A. 83.063824 (2011).

[21] https://en.wikipedia.org/wiki/Full_width_at_half_maximum.

[22] C. Cohen-Tannoudji, J. Dupont-Roc, G. Grynberg, Atom-Photon Interactions, John Wiley & Sons, (1998).

[23] G. Lindblad, Commun. Math. Phys. 48 (2), 119 (1976).

[24] M.M. Ćurčić, T. Khalifa, B. Zlatković, I.S. Radojičić, A.J. Krmpot, D. Arsenović, B.M. Jelenković, M. Gharavipour, Phys. Rev. A, 97, No. 6, 063851 (2018).

[25] J. A. Kleinfeld, A. D. Streater, Phys. Rev. A 53, 1839 (1996).

[26] Ken-ichi Harada, Kenji Mori, Junji Okuma, Nobuhito Hayashi, and Masaharu Mitsunaga, Phys. Rev. A, 78, 013809 (2008).

[27] Jinghui Wu, Yang Liu, Dong-Sheng Ding, Zhi-Yuan Zhou, Bao-Sen Shi, and Guang-Can Guo, Phys. Rev. A,87,013845 (2013).

[28] Nathaniel B. Phillips, Alexey V. Gorshkov and Irina Novikova, quant-Phys.09500340903159511 (2009).

[29] Andreas Lampis, Robert Culver, Balazs Megyeri, and Jon Goldwin,Phys. Optics 24, 015494 (2016).

[30] Robert W. Boyd, Daniel J. Gauthier, Alexander L. Gaeta, and Alan E. Willner, Phys. Rev. A, 71, 023801 (2005).

[31] M. M. Ćurčić, T. Khalifa, B. Zlatković, I. S. Radojičić, A. J. Krmpot, D. Arsenović, B. M. Jelenković, M. Gharavipour. " Four-wave mixing in potassium vapor with an offresonant double- system ", Phy. Rev. A, 97, 063851 (2018).

[32] D. Arsenović, M. M. Ćurčić, T. Khalifa, B. Zlatković, Ž. Nikitović, I. S. Radojičić, A. J. Krmpot, B. M. Jelenković. "Slowing 80-ns light pulses by four-wave mixing in potassium vapor", Phys. Rev. A, 98, 023829 (2018).

[33] Zhang, Guiyin, Haiping Li, Yidong Jin, and Hui Ji. "Investigation on the transparency of resonant absorption in the process of resonance-enhanced multiphoton ionization", j.optcom. 2013.06.026

[34] M. T. Turnbull, P. G. Petrov, C. S. Embrey, A. M. Marino, V. Boyer. "Role of the phase-matching condition in nondegenerate four-wave mixing in hot vapors for the generation of squeezed states of light", Phys. Rev. A, 88, 033845 (2013).

[35] J. Wang, Y. Wang, S. Yan, T. Liu, T. Zhang. "Observation of sub-Doppler absorption in the Λ-type three-level Doppler-broadened cesium system", Applied Physics B Lasers and Optics, s00340-003-1353-x (2004).

[36] J. Dimitrijević, D. Arsenović, B. M Jelenković "Coherent processes in electromagnetically induced absorption: a steady and transient study",

New Journal of Physics, Volume 13, (2011).

[37] Lee, Hee Jung, and Han Seb Moon. "Intensity correlation and anti-correlation in electromagnetically induced absorption", OE.21.002414, (2013).

[38] A. V. Taichenachev, A. M. Tumaikin, and V. I. Yudin. "Electromagnetically induced absorption in a four-state system", Phys. Rev. A, 61,011802 (1999).

[39] C. Goren, A. D. Wilson- Gordon, M. Rosenbluh, H. Friedmann. "Electromagnetically induced absorption due to transfer of coherence and to transfer of population", Phys. Rev. A, 67.033807 (2003).

[40] B. V. Zlatkovic, A. Krmpot, I. S. Radojicic, D. Arsenovic, M. Minic, B. M. Jelenkovic "Slow and stored light in amplifying four way mixing process", (ICTON), 7550577 (2016).

[41] Korociński, Jakub, Andrzej Raczyński, Jarosław Zaremba, and Sylwia Zielińska-Kaniasty. "Pulse propagation in atomic media in the triangular configuration", Journal of the Optical Society of America B. 30. 001517 (2013).

[42] Q. Glorieux, R. Dubessy, S. Guibal, L. Guidoni."Double-Λ microscopic model for entangled light generation by four-wave mixing", Phys. Rev. A, 82, 033819 (2010).

[43] I. Vadeiko, A. V. Prokhorov, A. V. Rybin, S. M. Arakelyan. "Nonlinear interaction of light with a Bose-Einstein condensate: Methods

to generate sub-Poissonian light", Phys. Rev. A, 72, 013804 (2005).

[44] B. Zlatković, A. J. Krmpot, N. Šibalić, M. Radonjić, and B. M. Jelenković. "Efficient parametric non-degenerate four-wave mixing in hot potassium vapor", Laser Physics Letters,12-2011/13/1/015205 (2016).

[45] M. M. Mijailovic, J. Dimitrijevic, A. J. Krmpot, Z. D Grujic, B. M. Panic, D. Arsenovic, D. V. Pantelic, B. M. Jelenkovic ."On non-vanishing amplitude of Hanle electromagnetically induced absorption in Rb", Opt.Express,15,001328(2007).

[46]Q. Zhongzhong, C. Leiming, J. Jietai. "Experimental characterization of quantum correlated triple beams generated by cascaded four-wave mixing processes", Applied Physics Letters,1,4921842 (2015).

[47] Taek Jeong, Han Seb Moon. "Phase correlation between four-wave mixing and optical fields in double Λ-type atomic system", Opt.Express,24,028774 (2016).

[48] Jinjian Du, Leiming Cao, Kai Zhang, Jietai Jing. "Experimental observation of multi-spatial-mode quantum correlations in four-wave mixing with a conical pump and a conical probe", Appl. Phys. Lett, 110, 241103 (2017).

[49] D. –S. Ding, Yun Kun Jiang, Wei Zhang, ZhiYuan Zhou, Bao-Sen Shi, Guang-Can Guo. "Optical Precursor with Four-Wave Mixing and Storage Based on a ColdAtom Ensemble", Phys. Rev. Lett,

144,093601(2015).

[50] Rong Ma, Wei Liu, Zhongzhong Qin, Xiaolong Su, Xiaojun Jia, Junxiang Zhang, Jiangrui Gao. "Compact sub-kilohertz low-frequency quantum light source based on four-wave mixing in cesium vapor", Opt. Lett, 37, 003141 (2018).

[51] H. –T. Zhou, Shao-Na Che, Yu-Hong Han, Dan Wang. "Influence of the frequency detuning on the four-wave mixing efficiency in three-level system coupled by standing-wave", Indian Journal of Physics, s12648-0117-1138-4 (2017).

[52] Hua Xu, Yuehui Lu, YoungPak Lee, Byoung Seung Ham. "Studies of electromagnetically induced transparency in metamaterials", Optics. Express,18,017736 (2010).